



REPORT DOCUMENTATION PAGE		L. REPORT NO. BuMines OFR 77-81	2.
4. Title and Subtitle A Model for the Determination of Flyrock Range as a Function of Shot Conditions		5. Report Date April 16, 1979	
7. Author(s) Julius Roth		8. Performing Organization Rept. No.	
9. Performing Organization Name and Address Management Science Associates Box 239 Los Altos, CA 94022		10. Project/Task/Work Unit No.	
		11. Contract(G) or Grant(G) No. (C) J0387242 (G)	
12. Sponsoring Organization Name and Address Office of the Director--Minerals Health and Safety Technology Bureau of Mines U.S. Department of the Interior Washington, DC 20241		13. Type of Report & Period Covered Contract research, 7/22/78--4/16/79	
15. Supplementary Notes Approved by the Director, Bureau of Mines, for placement on open file, May 22, 1981.		14.	
16. Abstract (Limit: 200 words) Flyrock is the source of most of the injuries and property damage in a majority of blasting accidents in surface mines. A quantitative correlation between shot conditions and maximum flyrock range can be used to define a blasting area in which no personnel or equipment should be present during a shot. The approach used was to develop a model that correlates shot conditions and initial flyrock velocities and permits computation of flyrock range from ballistic trajectories. The Gurney formula for velocity of explosively propelled plates or fragments was adapted to explosively propelled flyrock from vertical rock faces or from bench tops. The modified Gurney formula was then calibrated with measured flyrock velocities from mining and explosives literature. Charts were then developed for possible field use that gives maximum flyrock range as a function of shot conditions.			
17. Document Analysis a. Descriptors Surface mining Rock breakage Flyrock Explosives Safety Surface mine blasting b. Unrestricted/ Open-Ended Terms c. COSATI Field/Group 08I			
18. Availability Statement Release unlimited by NTIS.		19. Security Class (This Report) Unclassified	21. No. of Pages
		20. Security Class (This Page)	22. Price

REPRODUCED BY
U.S. DEPARTMENT OF COMMERCE
NATIONAL TECHNICAL
INFORMATION SERVICE
SPRINGFIELD, VA 22161



Acknowledgement

Several individuals who were neither employed by nor consultants to Management Science Associates (MSA) contributed to the success of this project. It is particularly gratifying to acknowledge the assistance given us by R. W. Watson, the Bureau of Mines Project Officer, who suggested the format of the charts for field use. Messrs. S. Winzer and V. Montenyohl of Martin-Marietta Laboratories, Baltimore, kindly provided us with unpublished data of their on-going photographic study of blasting in quarries. Dr. Per-Anders Persson of SveDeFo and Dr. A. Ladegaard-Pedersen of Nitro Nobel AB furnished us additional information on and clarification of several flyrock studies made in Sweden and Mr. P. Day of CIL did the same for studies made by CIL in Australia. Mr. V. Hooker of the Bureau of Mines, Denver, was most helpful in furnishing us with several hard-to-find reports of previous Bureau studies related to flyrock.

FOREWORD

This report was prepared by Management Science Associates, Los Altos, California, under USBM Contract No. J0387242. The contract was initiated under the Minerals Health and Safety Technology Program. It was administered under the technical direction of the Pittsburgh Research Center with Mr. Richard W. Watson acting as Technical Project Officer. Mr. William R. Mundorf was the contract administrator for the Bureau of Mines. This report is a summary of the work recently completed as a part of this contract during the period July 22, 1978 to April 16, 1979. This report was submitted by the authors on April 16, 1979. No patentable features are included in this report.





TABLE OF CONTENTS

Acknowledgement.	i
1.0 SUMMARY	1
2.0 INTRODUCTION.	3
3.0 QUANTITATIVE FORMULATION OF THE FLYROCK PROBLEM . . .	5
3.1 Ballistic Trajectories	5
3.2 Initial Flyrock Velocities from Vertical Faces.	6
3.2.1 Correlation of Powder Factors and c/m	10
3.2.2 Effect of Rock Properties	12
3.2.3 Effects of Multiple Boreholes	14
4.0 OBSERVED FLYROCK VELOCITIES AND THEIR COMPARISON WITH CALCULATIONS	18
4.1 Normalization of Flyrock Velocity Data	18
4.2 Flyrock Velocities from Vertical Faces	19
5.0 ESTIMATION OF MAXIMUM FLYROCK RANGE	25
5.1 Flyrock Ranges from Vertical Faces	25
5.2 Correlation of Observed Flyrock Range with c/m	27
5.3 Attempted Correlation Between Flyrock Range and Powder Factors	29
6.0 FLYROCK FROM BENCH TOPS	32
6.1 Model for Flyrock Velocities from Bench Tops (Cratering)	32
6.2 Flyrock Velocities from Bench Tops	35
6.3 Estimation of Flyrock Range from Bench Tops (Cratering)	39
6.4 Correlation of Bench Top Flyrock Range with c/m or Powder Factors.	39
6.5 Empirical Correlation Between Velocities of Bench Top Flyrock and Depth of Charge Burial	41



7.0	"WILD FLYROCK".	45
8.0	ESTIMATION OF FLYROCK RANGE FOR FIELD USE	48
8.1	Prior Attempts at Estimating Flyrock Range	48
8.2	Rationale for Field Use Charts for Flyrock from Vertical Faces.	52
8.3	Rationale for Field Use Charts for Flyrock from Bench Tops.	56
9.0	RECOMMENDATIONS FOR ADDITIONAL FLYROCK STUDIES.	58
10.0	REFERENCES.	61



LIST OF APPENDICES

A. ELEVATION CORRECTION FOR BALLISTIC TRAJECTORIES. 63

B. DERIVATION OF THE GURNEY EQUATION FOR A PLATE
DRIVEN BY A HEAD-ON DETONATION ORIGINATING AT A
RIGID WALL 65

C. CORRELATION OF THE GURNEY CONSTANT WITH DETONATION
VELOCITY 67

D. CHARTS FOR ESTIMATING MAXIMUM FLYROCK RANGE. 68

E. SOME CONSIDERATIONS OF THE UTILIZATION OF EXPLOSIVE
ENERGY IN BREAKING ROCK. 83

LIST OF FIGURES

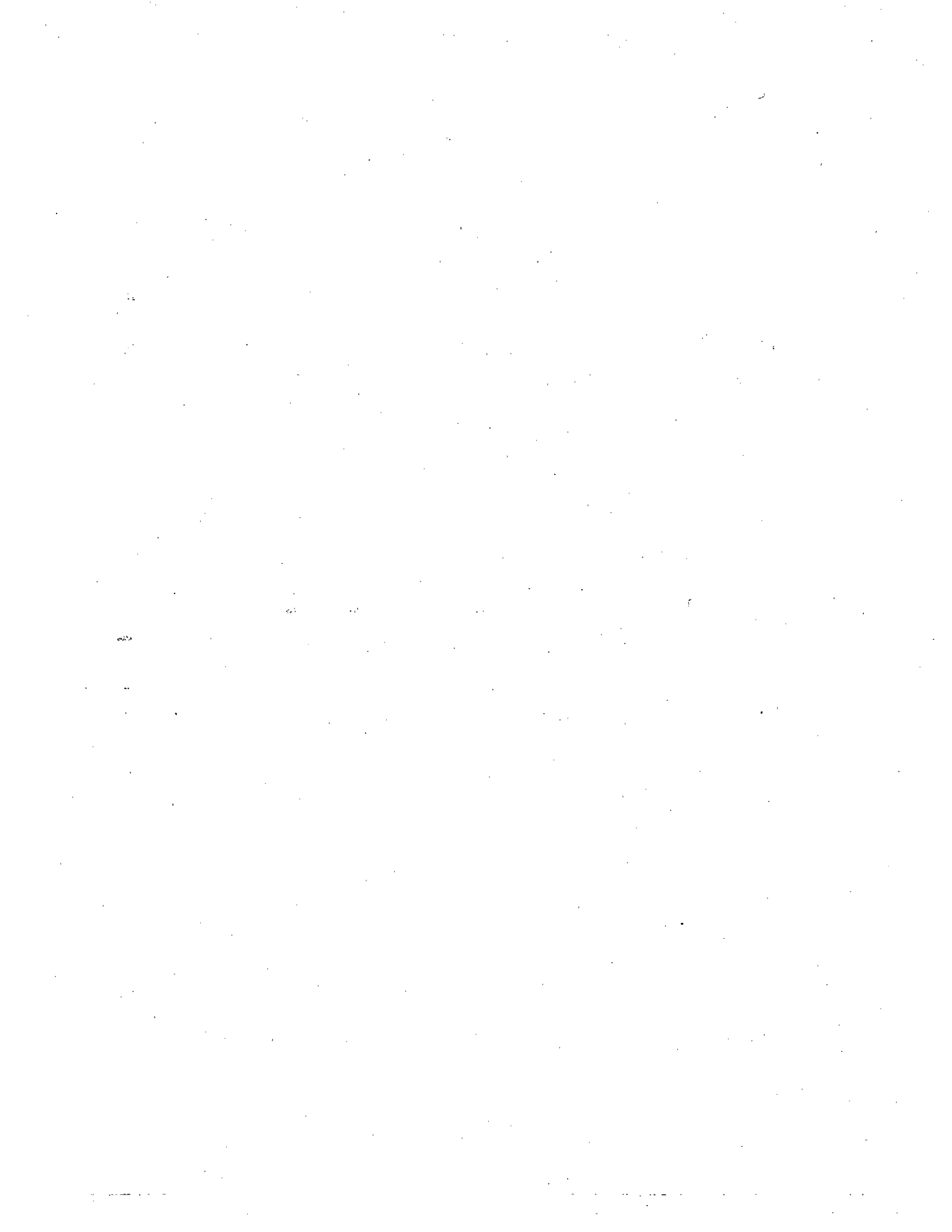
1a.	THREE-DIMENSIONAL VIEW OF A BENCH BLAST.	8
1b.	PLANE VIEW OF A BENCH BLAST.	8
2.	SCHEMATIC TOP-VIEW OF BENCH BLASTS WITH VARYING BOREHOLE SPACINGS.	15
3.	PLOT OF OBSERVED FLYROCK VELOCITY VS. c/m FOR BENCH SHOTS IN GRANITE	24
4.	CORRELATION OF FLYROCK RANGE OF BENCH BLASTS WITH c/m	28
5.	ATTEMPTED CORRELATION OF FLYROCK RANGE FROM BENCH BLASTS WITH POWDER FACTORS	30
6.	SCALED CRATER VOLUME AS A FUNCTION OF SCALED EXPLOSIVE CHARGE DEPTH	34
7.	EMPIRICAL CORRELATION OF BENCH-TOP FLYROCK WITH SCALED DEPTH OF CHARGE BURIAL	42
8.	FLYROCK RANGE FROM VERTICAL GRANITE FACES SHOT WITH ANFO OR SLURRY EXPLOSIVES.	55
1-D.	SKETCH OF A BENCH SHOT	69
2-D.	MAXIMUM RANGE OF VERTICAL FACE FLYROCK FROM ANFO-LOADED SHOTS IN GRANITE (FIXED BOREHOLE DIAMETERS)	70
3-D.	MAXIMUM RANGE OF VERTICAL FACE FLYROCK FROM ANFO-LOADED SHOTS IN SANDSTONE (FIXED BOREHOLE DIAMETERS)	71
4-D.	MAXIMUM RANGE OF VERTICAL FACE FLYROCK FROM ANFO-LOADED SHOTS IN LIMESTONE (FIXED BOREHOLE DIAMETERS)	72
5-D.	MAXIMUM RANGE OF VERTICAL FACE FLYROCK FROM ANFO-LOADED SHOTS IN GRANITE (FIXED BURDEN).	75
6-D.	MAXIMUM RANGE OF VERTICAL FACE FLYROCK FROM ANFO-LOADED SHOTS IN SANDSTONE (FIXED BURDEN).	76



7-D.	CORRELATION FACTOR ($s/W^{1/3}$) FOR BENCH TOP FLYROCK.	78
8-D.	MAXIMUM RANGE FOR BENCH TOP FLYROCK FOR ANFO-LOADED SHOTS IN GRANITE AND SANDSTONE	79
9-D.	ELEVATION CORRECTION FOR MAXIMUM FLYROCK RANGE.	81

LIST OF TABLES

1.	BREAKOUT ANGLES IN BENCH BLASTING.	9
2.	COMPARISON OF OBSERVED AND COMPUTED FLYROCK VELOCITIES IN GRANITE BENCH SHOTS.	20
3.	SPALL VELOCITIES IN GRANITE AND SANDSTONE.	23
4.	COMPARISON OF OBSERVED AND COMPUTED FLYROCK RANGES FOR FLYROCK FROM VERTICAL FACES	26
5.	COMPARISON OF OBSERVED AND COMPUTED FLYROCK VELOCITIES IN SANDSTONE CRATER SHOTS	36
6.	COMPARISON OF OBSERVED AND CALCULATED FLYROCK VELOCITIES FOR CRATER SHOTS IN GRANITE, LIMESTONE AND BASALT	37
7.	COMPARISON OF OBSERVED AND COMPUTED FLYROCK RANGES FROM BENCH TOPS	40
8.	COMPARISON OF EMPIRICAL AND GURNEY-MODEL FLYROCK RANGES FOR BENCH TOP FLYROCK	44
9.	"WILD" FLYROCK	46
10.	COMPARISON OF RULE OF THUMB AND OBSERVED FLYROCK RANGES FOR FLYROCK FROM "VERTICAL" FACES	49



1.0 SUMMARY

Flyrock is the source of most of the injuries and property damage in a majority of blasting accidents in surface mines. Since most of these accidents occur during normal blasting operations, there is a need to develop a quantitative correlation between shot conditions and maximum flyrock range. This maximum flyrock range can define a "blasting area" in which no personnel or equipment should be present during a shot. Such information can be of considerable value to pit foremen as well as to MSHA mine inspectors.

The approach used was to develop a model that correlates shot conditions and initial flyrock velocities and permits computation of flyrock range from ballistic trajectories. The Gurney formula for velocity of explosively-propelled plates or fragments was adapted to explosively-propelled flyrock from vertical rock faces or from bench tops. The modified Gurney formula was then "calibrated" with measured flyrock velocities from mining and explosives literature. Flyrock range thus computed was found to compare favorably with flyrock range in accident reports and with flyrock range obtained in one of our previous studies. Charts were then developed for possible field use which give maximum flyrock range as a function of shot conditions.

The model indicates that for flyrock from vertical faces, borehole diameter, minimum burden and height of explosive column define maximum flyrock range for a given explosive, shot in a given rock. Variation in flyrock range for different rock types under otherwise equivalent shot conditions, appears to be fairly small.

For flyrock originating from bench tops, flyrock range appears to be controlled by the distance of the top of the explosive column to the borehole collar, by total explosive load per borehole and, to a lesser extent, by borehole diameter. However, differences in flyrock range among different rock types

appear to be relatively large. The timing sequence of detonations of individual boreholes and gas venting during breakup of the vertical face may also affect top-flyrock range.

Recommendations for additional studies and analyses to confirm some of the conclusions of this study are presented. In particular the suggested additional studies are directed towards determining the causes of "wild" flyrock.

2.0 INTRODUCTION

By far the greatest single hazard in surface mine blasting operations is flyrock. Flyrock accounts for approximately half of all blasting-related accidents in surface mines (or somewhat more than one-third if fall of ground accidents are also included in blasting-related accidents).¹ Clearly, improved blasting practices and more definitive blasting regulations are still needed to minimize the flyrock hazard. The current study is aimed primarily at developing a flyrock model that may assist in the development of such regulations.

Section 57.2 of MESA's Metal and Nonmetal Health and Safety Regulations (CFR 30) defines blasting area as "the area near blasting operations in which concussion or flying material can reasonably be expected to cause injury." Note that this definition is entirely qualitative. It gives the blasting foreman no clue on how far to move personnel and equipment from the blast. Section 57.6-160 states: "Ample warning shall be given before blasts are fired. All persons shall be removed from the blasting area unless suitable shelters are provided to protect men endangered by concussion or flyrock from blasting." The second part of this regulation is difficult to enforce because a quantitative definition of blasting area is lacking. Clearly, Federal or State inspectors at present have no adequate means* of checking compliance with 57.6-160 and similar state regulations. Thus, the development of a quantitative definition of blasting area for normal shots is highly desirable.

* Certain rules-of-thumb now used for estimating flyrock range will be discussed in Section 8.1.

Air shock velocities (concussion) attenuate much more rapidly than flyrock velocities. Thus, it is entirely suitable to define the blasting area as the circle whose radius represents the maximum flyrock range for the particular conditions of the blast. In many instances (e.g., a high face behind the bench being shot or proper borehole layout and shot delay sequence) the actual danger area is the hemi-circle in front of the free face. However, the real problem is not whether to define the blasting area in terms of a circle or a hemi-circle, but in determining the conditions for the maximum flyrock range.

Certain conditions, such as inadequate burden, inadequate stemming, improper shot delay sequencing, or faults in the rock, etc., can produce a "wild" shot which throws flyrock much further than a "normal" shot. Obviously wild shots can be extremely hazardous. Thus, attempts at defining the conditions that may result in wild shots are included in the present study.

3.0 QUANTITATIVE FORMULATION OF THE FLYROCK PROBLEM

The approach used in the present study is to relate initial flyrock velocity to shot conditions and then use ballistic trajectories to compute maximum flyrock range. This approach is entirely justified because the effects of air friction are quite small for typical flyrock sizes and velocities. Furthermore, since safety is the prime consideration, it is the maximum flyrock range that defines a safe blast area, and in a ballistic trajectory the maximum range is obtained with flyrock propelled at an initial angle of 45°. Thus, determination of initial flyrock velocity completely determines maximum flyrock range.

In Section 3.1 we list the standard and slightly modified ballistic trajectory equations. Section 3.2 develops relationships between initial flyrock velocity and shot parameters for flyrock from vertical faces (highwalls). The problem of flyrock from bench tops (sometimes called cratering) will be addressed in Section 6.

3.1 Ballistic Trajectories

For flyrock at an initial velocity v_0 and an initial angle θ , the horizontal range L (i.e., return of the projectile to its original elevation) is given by

$$L = \frac{v_0^2 \sin 2\theta}{g} \quad (1)$$

where g is acceleration of gravity. Maximum flyrock range L_m is obtained when $\theta = 45^\circ$, or

$$L_m = v_0^2/g. \quad (2)$$

If the flyrock originates at an elevation of h above ground level, then (as shown in Appendix A) the maximum range L'_m for return of the projectile to ground level is given by

$$L'_m = \frac{L_m}{2} (\sqrt{1 + 4h/L_m} + 1). \quad (3)$$

Other equations which will be useful in the interpretation of some of the data are:

$$t_m = \frac{v_o \sin^2 \theta}{g} \quad (4)$$

where t_m is the time for the projectile to reach its maximum elevation h_m , and

$$h_m = \frac{v_o^2 \sin^2 \theta}{2g}. \quad (5)$$

3.2 Initial Flyrock Velocities from Vertical Faces

The Gurney formula² successfully predicts initial velocities of metal plates and metal fragments propelled by explosives.³ Consequently, it is logical to attempt to adapt the Gurney approach to the determination of initial velocities of rocks propelled by explosives, or more specifically, to flyrock velocities obtained in bench blasting.

The general form of the Gurney equation is

$$v_o = \sqrt{2E} f(c/m) \quad (6)$$

where $\sqrt{2E}$, the so-called Gurney constant, is characteristic of the explosive used; c and m respectively are the masses (total, or per unit length, or per unit area) of explosive and material that is propelled; the form of the function f depends on the geometry of the system. It will be shown later that initial flyrock velocity correlates much better with c/m than with more familiar terms such as powder factors.

Figure 1a is a schematic representation of the rock breakout produced by the detonation of one borehole of a typical bench blast, with explosive column length l , stemming length s , and burden to the free face b . Shot conditions are assumed to be such that breakout occurs only at the "vertical" free face in the region of length l . We idealize the situation by considering that the homogeneous rock surrounding the borehole acts as a "rigid wall" in all directions except that of breakout to the free face. This breakout per borehole has the shape of a prism. Also shown is the total volume of the rock broken (parallelepiped) that is conventionally used in computing powder factors. In Figure 1a it was assumed that the breakout angle is 90° , thus the breakout width at the free face is $2b$. If this angle is α rather than 90° , the breakout width at the free face is $2b \tan(\alpha/2)$. Then, per unit length of loaded borehole:

$$c/m = \frac{W/l}{\rho_m b^2 \tan(\alpha/2)} \quad (7)$$

where W/l is the explosive weight per unit length of borehole and ρ_m is the density of the rock. That α is indeed close to 90° is shown in Table 1. The α 's in this table are based on measurements of the amount of rock broken, but are certainly overestimated as explained in footnote a/ of this table.

For flyrock from the vertical face (see Figure 1b) and for the geometry of the system considered (as shown in Appendix B)

$$v_o = \sqrt{2E'} \sqrt{c/m} \quad (8)$$

where $\sqrt{2E'}$ is slightly less than $\sqrt{2E}$ because the direction of detonation is tangential to the rock and not head-on as in the derivation in Appendix B. The relation between $\sqrt{2E}$ and $\sqrt{2E'}$ was examined by the writer³ who also showed that for most explosives

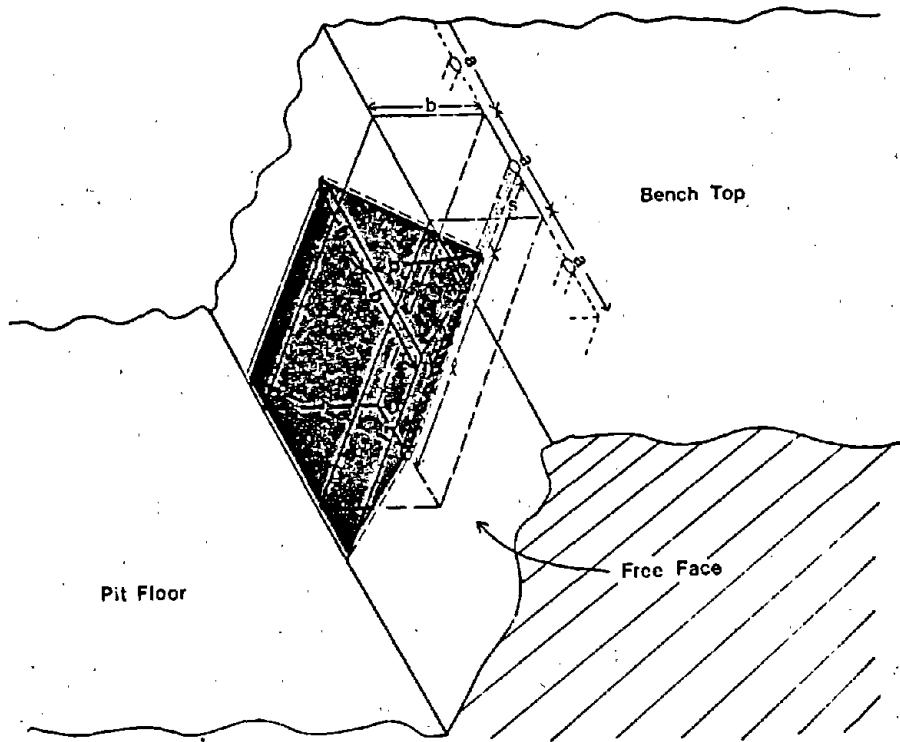


Figure 1a: THREE-DIMENSIONAL VIEW OF A BENCH BLAST

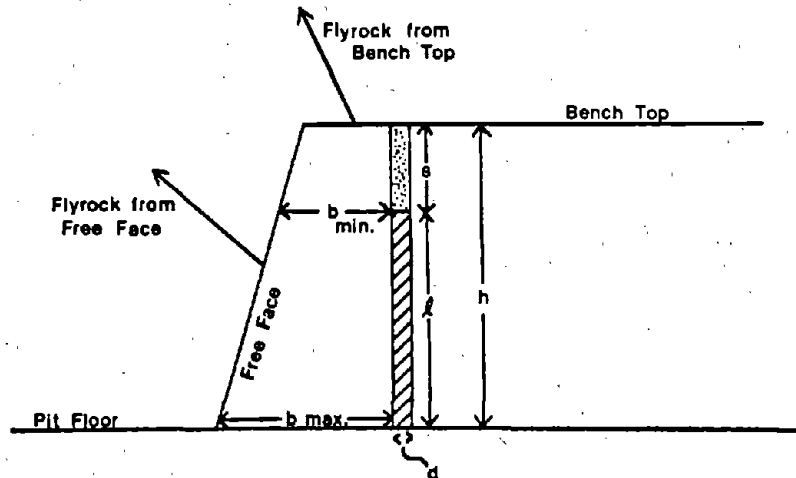
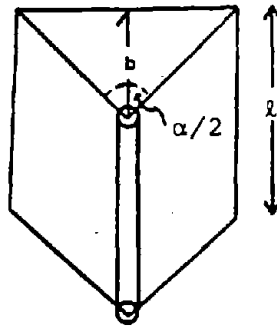


Figure 1b: PLAN VIEW OF A BENCH BLAST



<u>Source</u>	<u>b</u> <u>(cm)</u>	<u>d</u> [*] <u>(mm)</u>	<u>α</u> <u>(°)</u>	<u>W</u> <u>(g)</u>	<u>Rock</u>
Noren (Ref. 4)	17.8	38.1	100 ^{a/}	9.2 ^{b/}	Granite
"	22.9	"	110 ^{a/}	"	"
"	27.9	"	100 ^{a/}	"	"
"	33.0	"	90 ^{a/}	"	"
"	40.6	"	90 ^{a/}	"	"
"	53.3	"	95 ^{a/}	"	"
"	91.4	"	120 ^{a/}	"	"
Ladegaard-Pedersen (Persson (Ref. 5))	45.0	27.0	108 ^{a/}	15.0	Granite
"	"	"	" ^{a/}	20.0	"
"	"	"	" ^{a/}	30.0	"
"	"	"	" ^{a/}	35.0	"
"	"	"	" ^{a/}	40.0	"
"	"	"	" ^{a/}	50.0	"
"	45.0	"	" ^{a/}	85.0	"
"	40.0	"	106 ^{a/}	"	"
"	35.0	"	104.5 ^{a/}	"	"

* d = borehole diameter.

a/ Assumed rock broke out at uniform angle over entire hole depth.
If, as expected, break is beyond hole depth, above α's are too large.

b/ g/cm

Table 1: BREAKOUT ANGLES IN BENCH BLASTING

$\sqrt{2E'} = D/3$ where D is the detonation velocity of the explosive. However, for ANFO, which is the explosive used in most surface mine blasts, $\sqrt{2E'} = 0.44D$ (see Appendix C). In what follows we will use

$$v_o = 0.44D\sqrt{c/m} \quad (9)$$

for ANFO shots and

$$v_o = \frac{D}{3} \sqrt{c/m} \quad (10)$$

for most of the other shots.

All of the above refers to shots in a single borehole. Interactions between boreholes will be examined later.

3.2.1 Correlation of Powder Factors and c/m

The mining industry and regulatory personnel commonly express the amount of explosive required to obtain the desired rock breakage in terms of a quantity known as the Powder Factor. Usually, powder factors are expressed in pounds of explosive per cubic yard of rock to be broken. In open pit quarries or metal mines, powder factors usually range from about 0.6 to 2.3 pounds/cubic yard and are often around 1.3 pounds/cubic yard.⁶ In surface coal mines, powder factors are generally less and range from about 0.2 to 1.2 pounds/cubic yard and are often around 0.6 pounds/cubic yard.⁷

The method of computing powder factors is illustrated in Figure 1a. The volume of rock assumed to be broken by the detonation of each borehole ($a \times b \times h$) is indicated by parallelepiped shown in Figure 1a. Thus for a borehole charge of weight W, the powder factor is W/abh with W in pounds and the linear dimensions in yards. Combining this expression with the

definition of c/m , in Equation (7), for $\alpha/2$ assumed to be 45° , gives:

$$\text{Powder Factor} = \rho_m (c/m) (\ell/h) (b/a)$$

where ρ_m is in pounds/cubic yard. Depending on face height, explosive used and the degree of fragmentation desired, the ratios ℓ/h and b/a can vary appreciably from mine to mine even in mines mining essentially the same type of material. This introduces considerable uncertainty in any general correlation between powder factor and c/m based solely on ρ_m . A rough generalized relation is:

$$\text{Powder Factor} = 0.5\rho_m (c/m)$$

for shallow benches and

$$\text{Powder Factor} = 0.8\rho_m (c/m)$$

for deep benches. In each case the numerical factor is an "average" ℓ/h and it is assumed that $b = a$. Further complications arise from the fact that the b used in computing powder factors for a multi-row shot is usually the burden between rows of holes, whereas the appropriate b for computing c/m for maximum flyrock velocity is the minimum burden from any explosive loaded portion of a front-row borehole to the free face (see Figure 1b).

As will be shown in Section 6.0 flyrock from bench tops appears to be controlled by the distance s from the borehole collar to the top of the explosive column and the total weight W of explosive in the borehole. The controlling factor appears to be $s/W^{1/3}$. There is no simple correlation between this factor and the usual powder factor.

The model of Section 3.2 predicts a simple relation between initial velocity of flyrock from vertical faces and c/m . This relation is confirmed by measured flyrock data to be presented

in subsequent sections of this report. Since there is no "universal" correlation between the usual powder factor and the appropriate c/m , it is to be expected that there is no "universal" quantitative correlation between powder factors and flyrock. This is especially true of flyrock from bench tops. In a qualitative sense, it is to be expected that, in general, shots with large powder factors will produce more flyrock than shots with small powder factors. Clearly such qualitative statements are only of very limited value for establishing a safe blasting area for a particular set of shot conditions.

We will return to the question of correlation of flyrock and c/m or powder factors in Sections 5.3 and 6.4.

3.2.2 Effect of Rock Properties

In the derivation of equation (8) (see Appendix B) we ignored any energy-consuming effects other than those required to impart kinetic energy to the flyrock and the detonation product gases. Obviously, this is an oversimplification since rock fracture consumes some of the available chemical energy of the explosives. Similarly, generation of seismic waves in the rock, and the formation of the crushed rock zone immediately around the borehole, also consume energy. Rock breakage (at least most of the breakage), seismic wave generation and crushed zone formation are substantially complete before the breakout rock mass attains the velocity v_0 (see Appendix E and Refs. 8 and 9). Thus, correction terms for these energy losses must be introduced into equations (8) (9) or (10).

For a given homogeneous rock blasted with a given explosive, one might expect that the:

1. energy consumed in rock fracture is proportional to m ;
2. seismic energy is proportional to c ;
3. energy to form the crushed zone is proportional to c .

Assumptions 2 and 3 are fully justified by the data in references 10 and 11 and reference 9, respectively. Assumption 1 is more difficult to justify. The energy to fracture homogeneous rock should really be proportional to the number of fragments into which the mass of rock breaks, or more properly to the new surfaces created by fracture. However, inter-fragment friction during break-up and possibly plastic deformation of the fragmented material will also absorb energy. If fracture produces approximately equidimensional fragments, assumption 1 is valid. If the number and size of fragments varies greatly with shot dimensions (even though a given explosive is used to blast a given rock mass), assumption 1 is invalid. In the limit of large burdens and small charges it is known that shots break rock into large chunks or slabs, whereas under normal production blasting, rock is fragmented into many roughly equidimensional pieces.¹² Clearly, assumption 1 can be valid only over a limited range of m/c. Hopefully, it is valid over the "normal" range of m/c in production blasting.

Taking into account the above energy losses, equation (B-4) of Appendix B has to be modified as follows:

$$cE' - c(K_1W_S + K_2W_C) - m(K_3W_R) \approx \frac{1}{2}mu_0^2 \quad (11)$$

where W_S = seismic energy generated by a unit weight of explosive

W_C = energy to crush a unit weight of rock

W_R = energy absorbed in breaking out a unit weight of rock

K_1, K_2, K_3 are proportionality constants.

According to equation (11)

$$u_0^2 \approx 2E'(c/m) - 2K_3W_R - 2(K_1W_S + K_2W_C)c/m$$

or

$$u_0^2 \approx 2E'\left(\frac{c}{m}\right) \left[1 - \frac{K_1W_S + K_2W_C}{E'} \right] - 2K_3W_R \quad (12)$$

According to equation (12), a plot of v_0^2 vs. c/m should give a straight line of slope $2E' \left(1 - \frac{K_1 W_S + K_2 W_C}{E'}\right)$ and intercept of $-2K_3 W_T$. In what follows $\sqrt{2E'}$ will be replaced by $0.44D$ or $D/3$ depending on whether the main explosive charge is ANFO or any other explosive.

3.2.3 Effects of Multiple Boreholes

Consider a series of shots in which spacing between vertical boreholes, all of diameter d , is $2/3b$, b , and $4/3b$ as shown in a top-view sketch in Figure 2. In every case assume that hole (1) fires $1/2$ second before hole (2) and also assume that the breakout angle is 90° . For a "typical" round, the rock broken by hole (1) will have moved some 10 - 20 feet from its original position, thus creating a new free face for hole (2). The new minimum burdens for hole (2) are respectively $0.471b$, $0.707b$, and $0.943b$ for conditions (a), (b), and (c) in Figure 2. Obviously, condition (a) has the potential of throwing rock four times further than condition (c) since (from equations 2, 7, and 8) it can be shown that the maximum flyrock range, L_m , is proportional to $(d/b)^2$.

Normally, the delay between adjacent holes in the front row of a shot is much less than $1/2$ second. Thus, displacement of the rock broken by hole (1) (still assumed to fire before hole (2)) is much less than in the above examples. Also hole (2) fires (in part) into a "curtain" of broken and expanding rock. Nevertheless, because commercial delay devices can occasionally be erratic, it is desirable from the point of view of minimizing flyrock to maintain borehole spacing $\geq 4/3b$, so that even gross mistiming does not create very small burdens between adjacent boreholes. Unfortunately, this can result in poor fragmentation. Thus, some compromise is necessary.

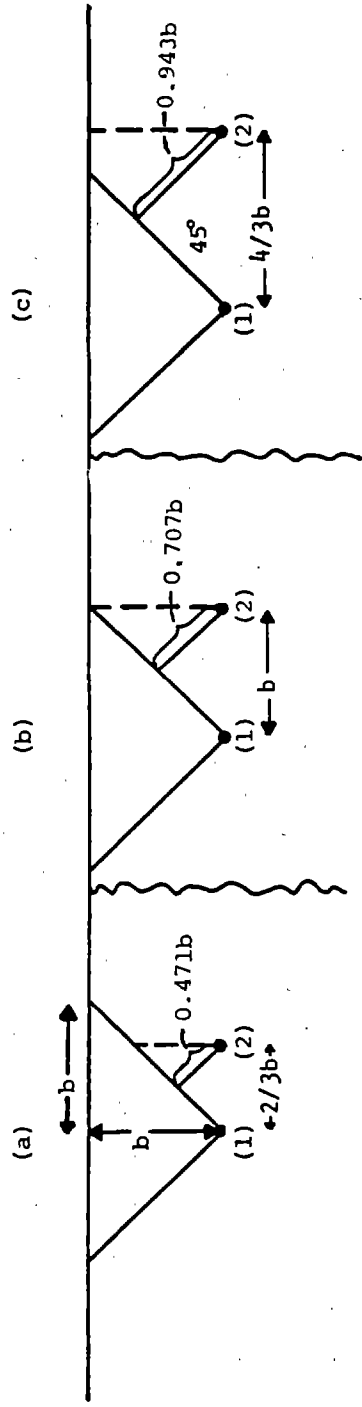


Figure 2: SCHEMATIC TOP-VIEW OF BENCH BLASTS WITH VARYING BOREHOLE SPACINGS

Above, we examined the potentially dangerous effects of multiple-hole bench blasting. However, under proper conditions multiple-hole shooting may actually reduce flyrock range. This is so because properly delayed multiple-hole shots will produce more fragmentation than the same shots fired "instantaneously". In these delayed shots it is likely that more of the chemical energy of the explosive is used in fragmentation processes than in the instantaneous shots and less energy is thus available to propel the broken rock. Quantitative formulation of this effect will be very difficult, but experimental corroboration is available from the studies of Forsberg and Gustavsson¹³, who found that instantaneous rounds throw rock further than short-period delay rounds.

These compensating effects suggest that, in the absence of unduly long delays between neighboring holes, highwall flyrock ranges from single holes or multiple holes can be substantially equivalent.

There is fairly wide-spread belief that improper delay sequencing can result in excessive flyrock from unrelieved back row holes. Under favorable conditions, this may indeed happen and produce "wild" flyrock and certainly flyrock in unexpected directions. The rationale for this belief is as follows. If a back row hole shoots before the holes in front of it have detonated and moved some of the rock between it and the free face, the effective burden on the back row hole is so large that it cannot be broken by the detonation of the back row hole. Consequently, this detonation is "relieved" by producing excessive "cratering" (and flyrock) at the top of the bench. However, such a sequence of events is limited to conditions for which the explosive load is less than a "critical" depth below the bench top. With sufficient stemming, both actual blasting experience* and experiments¹⁴.

* The writer witnessed a production shot in an open pit coal mine in which 9 holes were fired within a few seconds of each other without any apparent "relief" at the vertical face or bench top. Each hole contained about 1,500 lb. of ANFO but had 40 feet of stemming and an average burden of 38 feet.

indicate that there will be no such cratering even in the absence of any nearby free face other than the bench top. Flyrock from bench tops will be considered in Section 6.

4.0 OBSERVED FLYROCK VELOCITIES AND THEIR COMPARISON WITH CALCULATIONS

The flyrock measurements that we were able to find in the literature fall into the following categories:

1. Flyrock from vertical faces for granite. These data cover a wide range of c/m and a wide range of detonation velocities, D. These are the most reliable data we have.
2. Flyrock from vertical faces for dolomite and limestone. Here both c/m and D ranges are relatively narrow and the data are discordant.
3. Somewhat discordant data for crater shots in sandstone. A few of the c/m values here are subject to the uncertainties discussed in Section 6.1. The range of detonation velocities is reasonably wide.
4. Scanty data for flyrock from granite and limestone bench tops. Both c/m and D ranges for these data are very limited.

Items 3 and 4 will be discussed in Section 6.

4.1 Normalization of Flyrock Velocity Data

We shall use equation (12) to compare measured and computed flyrock velocities. According to equation (12) a plot of the measured velocity squared (v_{obs}^2) vs. c/m should be linear with a slope of $2E' \left(1 - \frac{K_1 W_s + K_2 W_c}{E'}\right)$ and an intercept of $-2K_3 W_r$, provided that all velocity measurements are made with the same explosive. If measurements made with several different explosives are to be compared with theory, some method of normalizing the measured velocity data must be developed. It will be shown in Appendix 7.1 that the observed velocities can be normalized to a common $2E'$ or to a common D^2 since $2E'$ is directly proportional to D^2 . To illustrate this normalization scheme, suppose that most of the velocity data for a given rock type is for a dynamite whose Gurney

constant $(\sqrt{2E'}) = D_1/3$ where D_1 is the detonation velocity of this dynamite for the conditions of the measurement. No correction factor will be applied to the observed flyrock velocities generated with this explosive. Now suppose that ANFO at a detonation velocity of D_2 was used to obtain some of the velocity measurements in the above rock type. The normalization factor applied to these latter measurements (i.e., the factor by which u_{ANFO}^2 is multiplied) is:

$$\frac{2E'_{ANFO}}{2E'_{dynam}} = \frac{(0.44D_2)^2}{(D_1/3)^2}$$

4.2 Flyrock Velocities from Vertical Faces

We will illustrate the method of "proving-in" our computed flyrock velocities with flyrock data for granite. For each measured flyrock velocity datum we computed c/m via equation (7), or from the total amount of rock broken and the total explosive charge weight, whenever such data were available. If no information on the breakout angle α was available, it was assumed that $\alpha/2 = 45^\circ$ (see Table 1). A least-squares linear regression fit was then used to obtain the most probable values of the slope and intercept of a linear plot of measured flyrock velocity squared versus computed c/m. For each set of data points we also computed a correlation coefficient $r = S\sigma_x/\sigma_y$ where S is the linear regression slope and σ_x and σ_y are the standard deviations of the x and y values. A correlation coefficient approaching unity shows that the y and x values can indeed be represented by a linear relation.

Measured flyrock velocities and computed c/m's for granite are shown in Table 2. The linear regression slopes and intercepts for these data are as follows:

Granite: $u_o^2 = 3.487 \times 10^6 (c/m) - 584 \quad (m/sec)^2 \quad (13)$
 (17 data points; $r = 0.999$; normalized to $D/3 = 2300$ m/sec)

Data Source	Explosive	D/3 (km/sec)	Normalized* v_{obs}^2 (m/sec) ²	c/m x 10 ⁴	Computed [†] v_0^2 (m/sec) ²
Ref. 15	EL-506C	2.30	1050	4.68 ^{a/}	1109
"	"	"	234	2.25 ^{a/}	262
"	40%PETN/ NaCl	1.08	254	=2.18 ^{a/}	=237
"	60% "	1.50	174	=1.95 ^{a/}	=157
"	EL-506C	2.30	104 ^{b/}	1.96 ^{a/}	160
"	"	"	94 ^{b/}	1.80 ^{a/}	105
"	"	"	90.3	2.10 ^{a/}	209
"	"	"	24 ^{c/}	1.20 ^{a/}	-105
"	"	"	12.3 ^{c/}	0.72 ^{a/}	-272
Ref. 4	Dynamite	1.28	480	2.54	363
"	"	"	3730	11.70	3557
"	"	"	5695	18.32	5865
"	"	"	14500 ^{c/}	30.52	10119
"	"	"	8730 ^{c/}	36.64	12253
"	"	"	19150 ^{c/}	39.83	13366
"	"	"	28500	83.27	28513
Ref. 16	Gelamite D	1.995 ^{d/}	349	2.53	359
"	"	"	753	3.17	582
"	"	"	1202	4.93	1196
Ref. 5	Dynamex	1.00	3885	12.86	3961
"	"	"	2304	9.92	2936
"	"	"	4826	17.32	5576
Ref. 17	ANFO	2.07 ^{f/}	278 ^{e/c/}	2.10	209
Ref. 18	---	---	=0 ^{g/c/}	=1.9 ^{f/}	=140

* Normalized to D/3 = 2.30 km/sec $\ddagger v_0^2 = 3.487 \times 10^6 (c/m) - 584$.

a/ Ref. 12 gives explosive weight W and the total weight of rock broken m_t ; $c/m = (\frac{W}{m_t})(\frac{L_1}{h})$ where L_1 =length of borehole and h=height of rock.

b/ Charge diameter less than borehole diameter.

c/ Not used in computing slope and intercept.

d/ 0.38D

e/ Shots in hematite ore.

f/ 0.44D

g/ It is claimed that maximum burden to borehole diameter ratio to break rock is 46. In computing c/m for this ratio we assumed $\rho_c/\rho_m = 1/2$

Table 2: COMPARISON OF OBSERVED AND COMPUTED FLYROCK VELOCITIES IN GRANITE BENCH SHOTS

When all the data in Table 2 are used, except those from References 17 and 18 and the two data points at the bottom of the group of data taken from Reference 15, $r = 0.971$ and

$$v_0^2 = 3.66 \times 10^6 (c/m) - 518 \quad (\text{m/sec})^2 \quad (13a)$$

All the data of Table 2 are plotted in Figure 3 to provide a visual confirmation of the validity of the proposed linear relation between v_0 and c/m . Note that the slope and intercept of the line based on all the data (Equation 13a) is quite similar to the slope and intercept of the line based on data from which three datum points have been omitted (Eq. 13).

The datum point labelled L&K (and the bottom entry in Table 2) is derived from Langefors¹⁶ claim that the maximum burden-to-diameter ratio to just barely break rock is 46. This ratio gives a $c/m = 1.9 \times 10^{-4}$ (from Eq. 7) and since it is claimed that rock is just barely broken $v_0^2 = 0$.

The scanty data for dolomite and limestone vary too much to permit determination of an accurate relationship such as the one in equation (13). Consequently, the following equation is at best an approximation:

Dolomite and Limestone: $v_0^2 \approx 3 \times 10^6 (c/m) - 200 \quad (\text{m/sec})^2 \quad (14)$
 (7 data points; normalized to $0.44D = 1880$ m/sec; References 16, 19, 20, and 21)

Examination of Table 2 reveals that for $c/m \leq 1.5 \times 10^{-4}$ equation (13) does not hold. Indeed the data of reference 12 show some half-dozen points in this region with finite flyrock velocities, whereas equation (13) predicts zero flyrock velocity. These low flyrock velocities in the region of $c/m \leq 1.5 \times 10^{-4}$ may be due to spalling. Spall velocities v_{fs} (i.e., free surface velocities) in the elastic range are given by

$$v_{fs} = 2c_0 \epsilon \quad (15)$$

where c_0 is the longitudinal sound velocity in the rock and ϵ is the strain in the rock at its free surface boundary. Table 3 shows that there is reasonable accord between spall velocities calculated by equation (15) and the observed fly velocities in the low c/m range. Note that all these velocities are quite low.

<u>Rock</u>	<u>Sound Velocity</u> $c_0 \times 10^{-3}$ (m/sec)	<u>Stress</u> $\sigma \times 10^{-7}$ (dynes/cm ²)	<u>Strain</u> $\epsilon \times 10^4$	<u>Free* Surface Velocity</u> v_{fs} (m/sec)	<u>Observed Velocity</u> (m/sec)
Granite	5.20	5.86	2.93 ^{a/}	3.0	1.8
"	"	8.45	4.23 ^{a/}	4.4	3.5
"	"	8.97	4.48 ^{a/}	4.7	4.9
"	"	14.5	7.25 ^{a/}	7.5	6.8
"	"	19.3	9.66 ^{a/}	10.0	9.5
Sandstone ^{b/}	1.32	-	2.0	5.3	5.8
"	"	-	2.0	5.3	4.0
"	"	-	1.5	4.0	2.7
"	"	-	1.2	3.1	=0

* $v_{fs} = 2c_0\epsilon$

a/ $\epsilon = \frac{\sigma}{Y}$ where Y is Young's modulus = 2×10^{11} dynes/cm² according to Ref. 14. σ from Ref. 15.

b/ Crater shots; ϵ from curves in Ref. 11.

Table 3: SPALL VELOCITIES IN GRANITE AND SANDSTONE

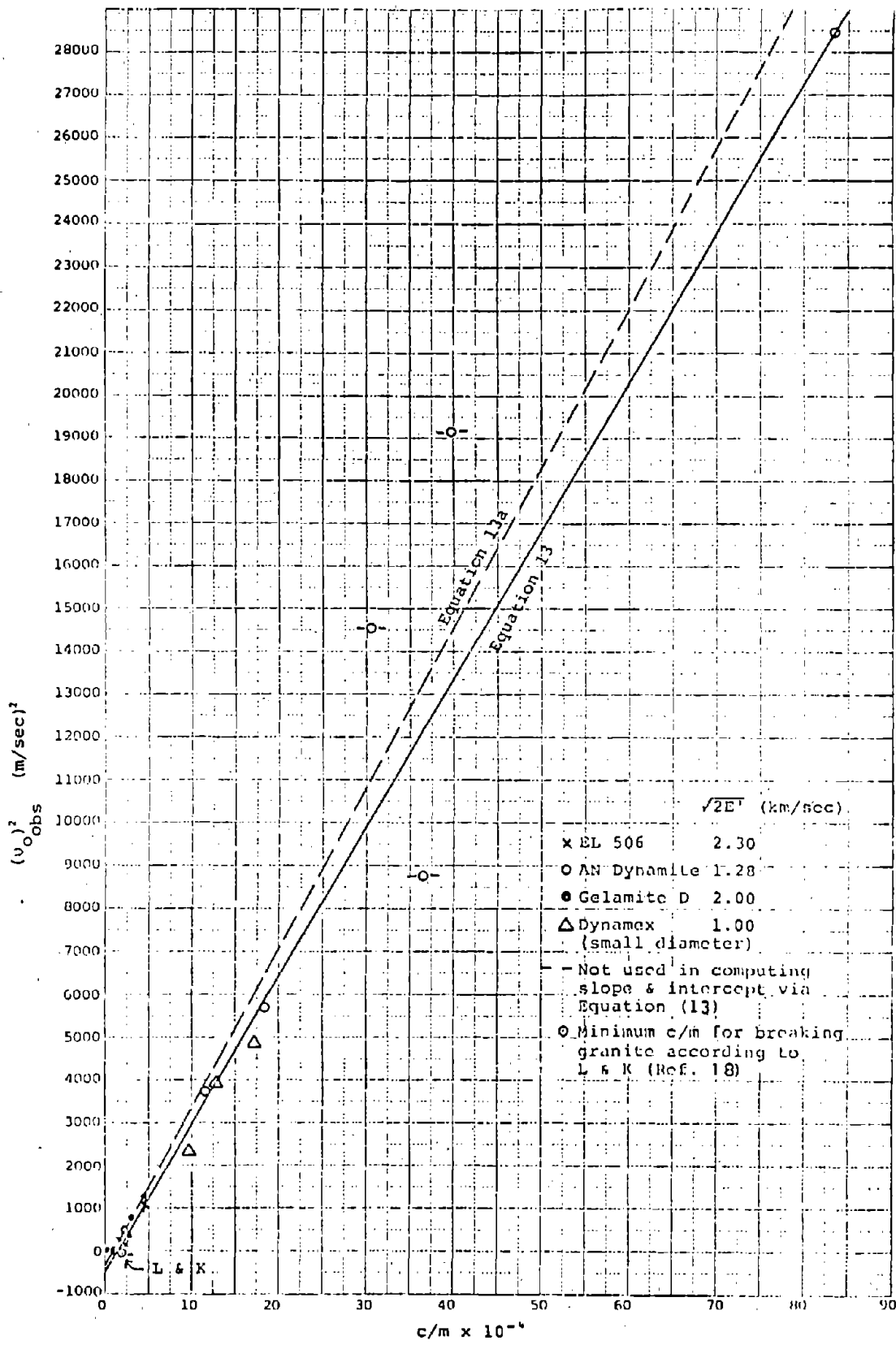


Figure 3: PLOT OF OBSERVED FLYROCK VELOCITY VS. c/m FOR BENCH SHOTS IN GRANITE

5.0 ESTIMATION OF MAXIMUM FLYROCK RANGE

In Sections 3.0 and 4.0 the groundwork was laid for a method of computing flyrock range as a function of shot characteristics. This method will be applied now to computing the maximum flyrock range of shots that were witnessed, or shots described in MESA accident reports. In our own observations¹ we know whether the flyrock originated primarily from the vertical face of a highwall or from the bench top. This information is lacking in the MESA reports and must be determined a posteriori from the computations.

5.1 Flyrock Ranges from Vertical Faces

Observed and computed flyrock ranges are compared in Table 4. In general, computed ranges should be equal to or greater than observed ranges, since in the computation it is assumed that the initial flyrock angle θ is 45° , but in reality this angle is usually either greater or less than 45° . Most "vertical" faces are not truly vertical. Consequently, the burden to the free face varies along the explosive column (see Figure 1b). The computed flyrock ranges in Table 4 are based on minimum burden whenever there was sufficient information to determine a minimum burden. In most MESA reports of blasting accident investigations the "burden" usually quoted is the separation between rows of holes. This "burden" can be different from the minimum, average, or maximum burden to the free face which are the burdens required for the computation. The MESA reports do not give the maximum flyrock range but only the distance from the shot to where the victim was located. Moreover, there is usually no indication how this distance was measured or estimated. Most of the observed flyrock ranges extracted from Reference 1 were obtained by scaling still-camera records of the various shots witnessed, but several ranges are "eye-ball" estimates made immediately after a shot. Incidentally, all the data in Table 4 are based on production shots in actual surface mines. None of these data are derived from experimental studies or exploration shots.

Minet	Rock	Borehole Diameter d (inches)	Burden b (feet)	Height of Explosive Column l (feet)	Weight of Explosive/Ft. W/l (lbs./ft.)	$\frac{W}{l^2}$ (lb./ft. ²)	\sqrt{W} (ft./sec)	$\frac{W}{l^2}$ (ft./sec ²)	L_m^* (feet)	L_m^{**} (feet)	L Obs (feet)
Arroyo Quarry	Granite	3	10	52 ^{a/}	4.6	0.29	6350 ^{b/}	3720	115	150	300-350
Mine J	Porphyry	9	27	10	27.8	2.18	6710	2019 ^{c/}	63	85	100
Mine P	Porphyry	7-7/8	25	15	16.7	1.53	6640	88 ^{c/}	3	8	50
Mine K	Diorite	9-7/8	27	25	32.6	2.71	6710	3532 ^{c/}	112	133	100
Mine X	Diabase	6-1/2	21	65	18.8	2.24	5550	2091 ^{c/}	65	107	100
Mine H	Taconite	9-23	44	26	210 ^{d/}	5.2	6200 ^{b/}	9577 ^{c/}	291	315	300-350
Mine D	Sandstone	6-1/4	18	12.5	11	2.42	6480	1738	54	64	50
Mine Y	Shale	9	12	20	22.5	11.17	6700	30115 ^{e/}	935	955	100
Mine C	Shale	15	35	70	50	2.5	6700	11340 ^{e/}	140	175	100
Mine B	Shale	15	38	46	70	3.5	7020	21115 ^{e/}	160	200	100
Holin Coal	Shale	5	12	5	3.0	3.5	6300	2423 ^{e/}	128	150	100
Roberson Coal	Shale	6-1/4	11 ^{f/}	9	11.3	4.8	6480	28465 ^{e/}	260	270	100
Mine W	Limestone	6-3/4	13	38	12	4.52	6380	14193	142	176	100
Mine V	Limestone	5-1/2	13	117	12	4.2	6550	13015	405	500	100
Mine U	Limestone	6-3/4	19	60	13	9.4	6580	132170	1000	1060	100
Carbon Limestone	Limestone	6-1/4	15	45	8.3	2.2	6480	5490	170	205	600 ^{g/}
Fernstead Quarry	Limestone	3-1/2	7	39	3.5	4.46	5750	10635	135	170	450 ^{g/}
Quarry	Limestone	3	8	56	4.23	3.78	4670 ^{h/}	5751	179	230	100
Mine R	Dolomite	6	12	50	11	4.24	6450	12650	199	435	250

* Same designations as in Appendix B of Reference 1. Data for named mines from MESA Reports.

^{a/} From Equation 2.

^{b/} From Equation 3 but with l substituted for h.

^{c/} Value shown is height of quarry face.

^{d/} Slurry explosives with $\sqrt{W} = D/3$; all others are ANFO with $\sqrt{W} = 0.4 D$.

^{e/} Used Equation 11.

^{f/} Average loading in a tapered borehole.

^{g/} Used Equation 16.

^{h/} Burden not given in report; estimated from bench width and number of rows.

^{i/} Flyrock from bench top.

^{j/} Semi-gal; D/3

Table 4: COMPARISON OF OBSERVED AND COMPUTED FLYROCK RANGES FOR FLYROCK FROM VERTICAL FACES

Taking into account the several uncertainties listed above, agreement between the observed and computed flyrock ranges shown in Table 4 is quite satisfactory. However, all computed values for flyrock ranges in limestone and dolomite shots should be considered to be provisional because of uncertainty in the values of the constants of Equation (14).

Note that only five of the 19 shots listed in Table 4 threw rock 400 feet or more. In at least one, and probably two, of these five shots the flyrock originated from the top of the bench and not from the vertical face. This may suggest that most "wild" (far-ranging) flyrock does not originate from vertical faces - an implication that will be examined in Section 7.0. A similar conclusion can be reached on the basis of Swedish studies (see Section 8.1).

5.2 Correlation of Observed Flyrock Range with c/m

The data of Table 4 are more readily assimilated if they are presented in graphical form. Examination of Equations (12) and (2) suggests that observed flyrock range (L_m) should be plotted as a function of c/m . This suggestion receives further support from the fact that most of the data in Table 4 is for shots with similar values of $\sqrt{2E^1}$. Consequently, in Figure 4 we have plotted observed flyrock range vs. c/m (data points). The three computed lines (from top to bottom) are plots of Equations (14), (17), and (13). Included in the plot are also flyrock ranges for flyrock from bench tops which will be discussed in Section 6.4. One important conclusion to be drawn from the plot in Figure 4 is that all but two of 21 data points for flyrock from vertical faces fall within the area of the "theoretical" lines or lie very near to them (one datum point, not shown in the plot, which lies within the area of

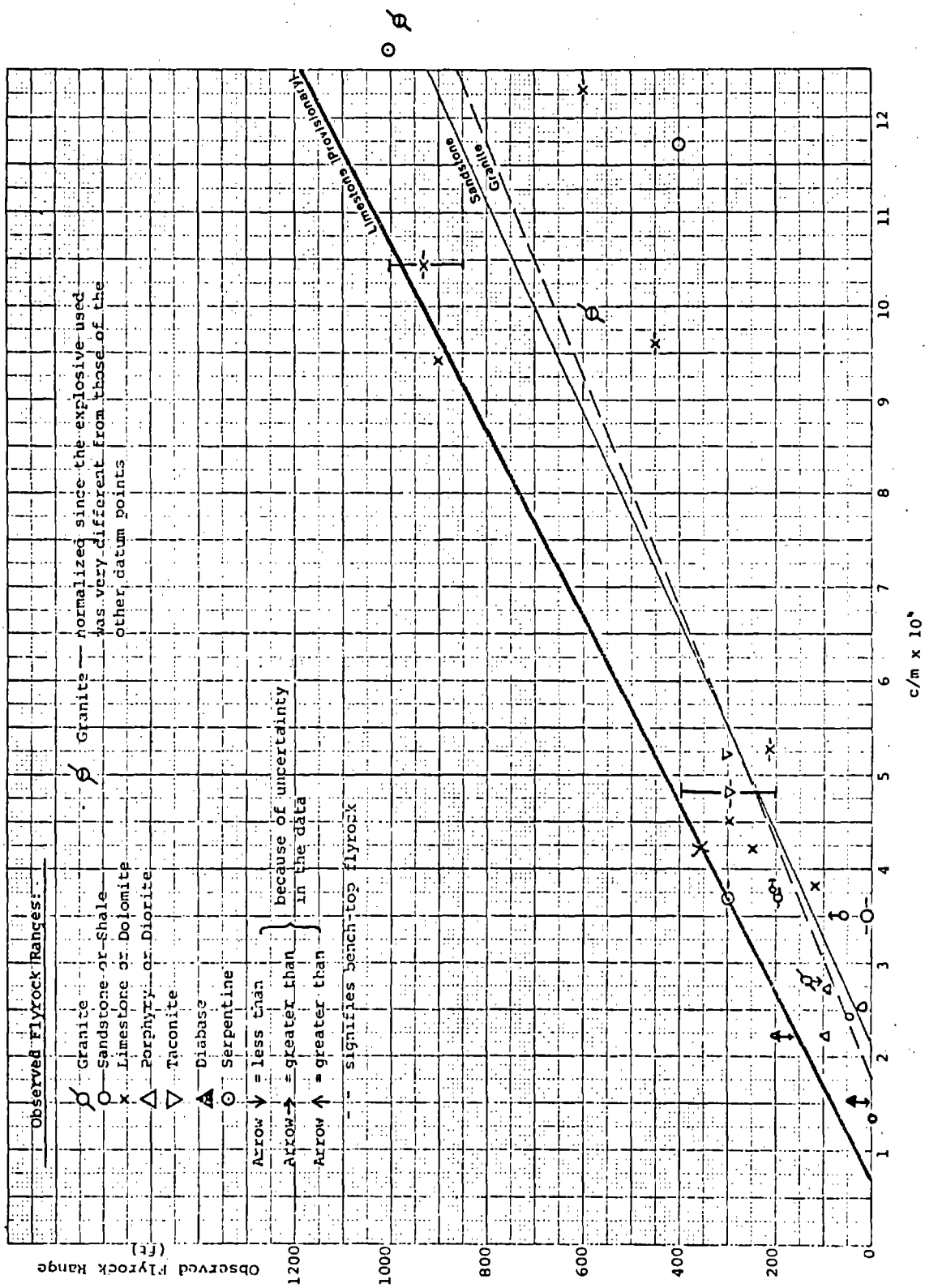


Figure 4: CORRELATION OF FLYROCK RANGE OF BENCH BLASTS WITH c/m

the lines is at $L_m = 1200$ feet and $c/m = 17.5 \times 10^{-4}$). An even more important conclusion is that none of the data points lie above the computed lines. This is very significant from a safety point of view since any viable flyrock model should err in overestimating rather than underestimating flyrock range. Three data points, taken from Reference 5 (one of these is not shown in the plot) involved the use of an explosive whose $\sqrt{2E^T}$ was substantially different from the $\sqrt{2E^T}$ values in Table 4. The observed flyrock range for these three points was normalized according to the procedure described in Section 4.1.

5.3 Attempted Correlation Between Flyrock Range and Powder Factors

It seems likely that field personnel would prefer to have flyrock range expressed as a function of something familiar like powder factors rather than the term c/m which is certainly not in common use in mining. Consequently we have attempted to make this correlation but were largely unsuccessful as discussed below.

Figure 5 presents the same data as Figure 4 but the abscissa is powder factor rather than c/m . The two computed lines shown are plots of Equation (14) (top) and Equation (13) (bottom) with c/m 's (in the equations) converted to powder factors via the relations given in Section 3.2.1, with the assumptions that $b = a$ and $l/h = 0.75$. Included in Figure 5 are data points for flyrock from bench tops which will be discussed in Section 6.4.

There are two important differences between the plots of Figure 4 and Figure 5. As discussed in Section 5.2, the correlation between flyrock range and c/m appears to be very good. The correlation between flyrock range and powder factor is much less satisfactory. For the latter (Figure 5), eight of the 21 data points for flyrock from vertical faces lie outside

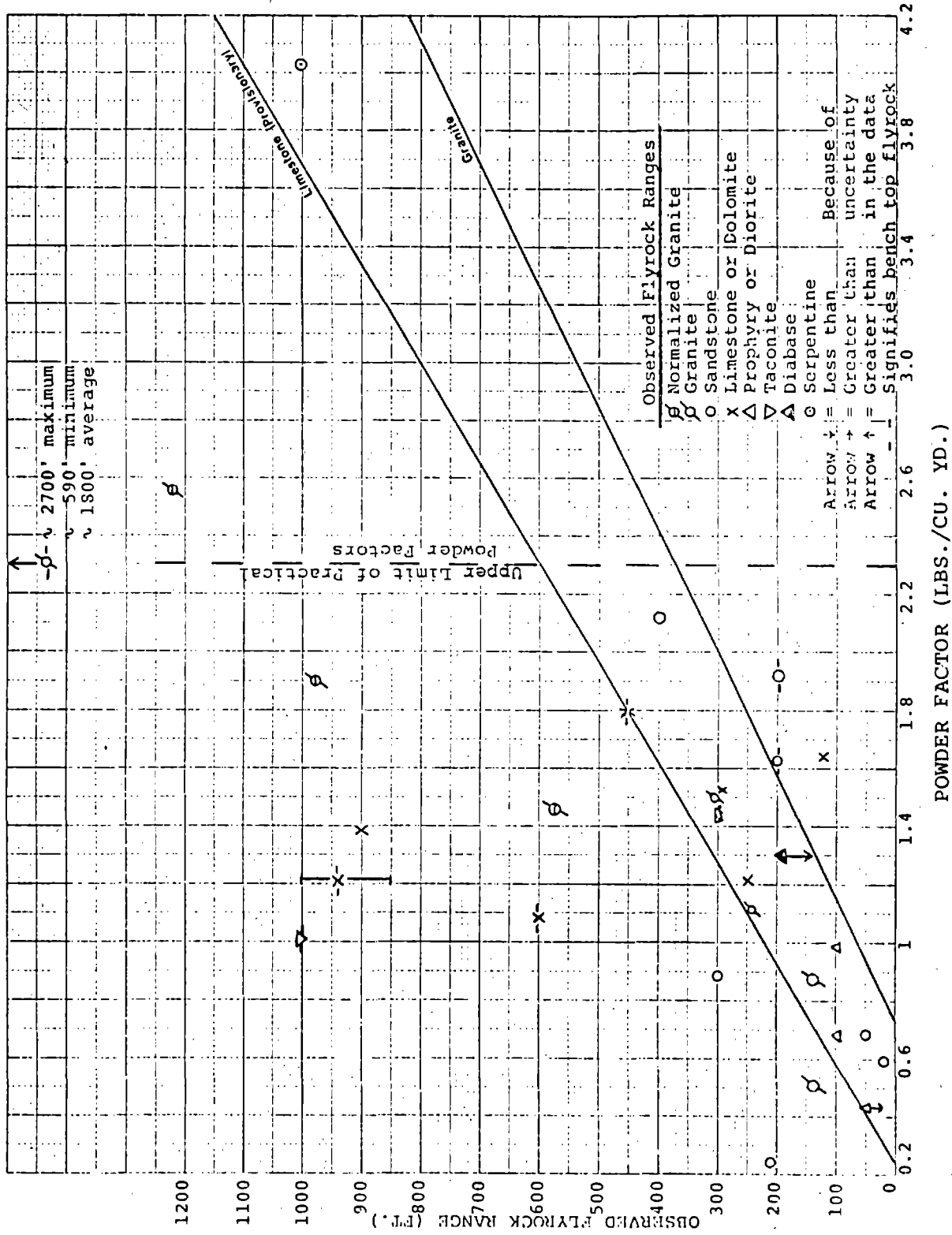


Figure 5: ATTEMPTED CORRELATION OF FLYROCK RANGE FROM BENCH BLASTS WITH POWDER FACTORS

the area between the two "theoretical" lines. Even more disturbing is the fact that six of these points lie well above the upper theoretical line. This means that a correlation based on powder factors tends to underestimate flyrock range. From a safety point of view such a correlation is bad unless the degree of underestimation is accurately known over the practical powder factor range.

6.0 FLYROCK FROM BENCH TOPS

In the preceding sections we have been considering flyrock that originates from a "vertical" free face. We will now examine conditions that can produce flyrock from "horizontal" free faces (bench tops). It will become quite apparent that quantitative treatment of this problem is more complex and the results obtained are less certain than those for flyrock from vertical faces.

6.1 Model for Flyrock Velocities from Bench Tops (Cratering)

There are two serious problems in adapting the Gurney approach to bench top flyrock, namely:

1. The assumption that the material surrounding the explosive charge acts as a "rigid wall" in all directions but those of material breakout is less plausible than the equivalent assumption for well-stemmed shots with vertical breakout.
2. The values of c/m are difficult to establish because crater dimensions (amount of material broken) go through a maximum that varies with explosive charge weight and the depth of the explosive charge below the bench top.

If the rigid wall assumption is valid, and if an appropriate c/m can be defined, the equations for the initial velocity of cratering shots are almost identical with those given for bench shots. The minor difference between these shots is that the Gurney constant is $\sqrt{2E}$ for a head-on detonation rather than $\sqrt{2E'}$ for the tangential detonation that obtains in vertical breakout³. Because of the potentially large uncertainties introduced by problem areas (1) and (2) above this minor difference will be ignored. To use these equations one needs to establish means of estimating c/m for crater shots. At present this can only be done empirically.

Duvall and Atchison¹⁴ showed that plots of V/W vs. $s/W^{1/3}$ give roughly bell-shaped curves for several different rocks blasted by several types of explosives (Figure 6). Here, V is crater volume, W is explosive charge weight, and s is depth of burial of the center of mass of a concentrated charge. Within the large scatter of their data, type of explosive does not appear to affect these curves for any given rock. The relation between V/W and c/m is as follows:

$$c/m = W/\rho_m V \quad (16)$$

where ρ_m is the density of the rock in lbs/ft^3 , if W is in pounds and V is in ft^3 . There are however two serious questions that need to be resolved before applying these data to the estimation of c/m . They are:

1. What is s for an elongated rather than concentrated charge?
2. Is it meaningful to use the portion of the curves to the right of their maxima?

A posteriori, it has been found that taking s as the distance from the bench top to the center of mass of an elongated charge (the kind usually encountered in bench blasting) leads to a gross underestimate of flyrock range. There is some ad hoc experimental justification for taking s as the distance to the top of an elongated charge, and then still use the experimental curves of V/W vs. $s/W^{1/3}$ that were obtained for s equal to the distance to the center of mass of a concentrated charge (see Table 7).

Use of curves beyond their maxima in estimating c/m and subsequently v_o leads to an absurdity. These curves show that for large $s/W^{1/3}$, V/W is small and above a critical value of $s/W^{1/3}$ no crater is formed. Since c/m increases as V/W decreases, use of V/W , taken from the branch of the curve where V/W is decreasing, predicts increasing flyrock velocities,

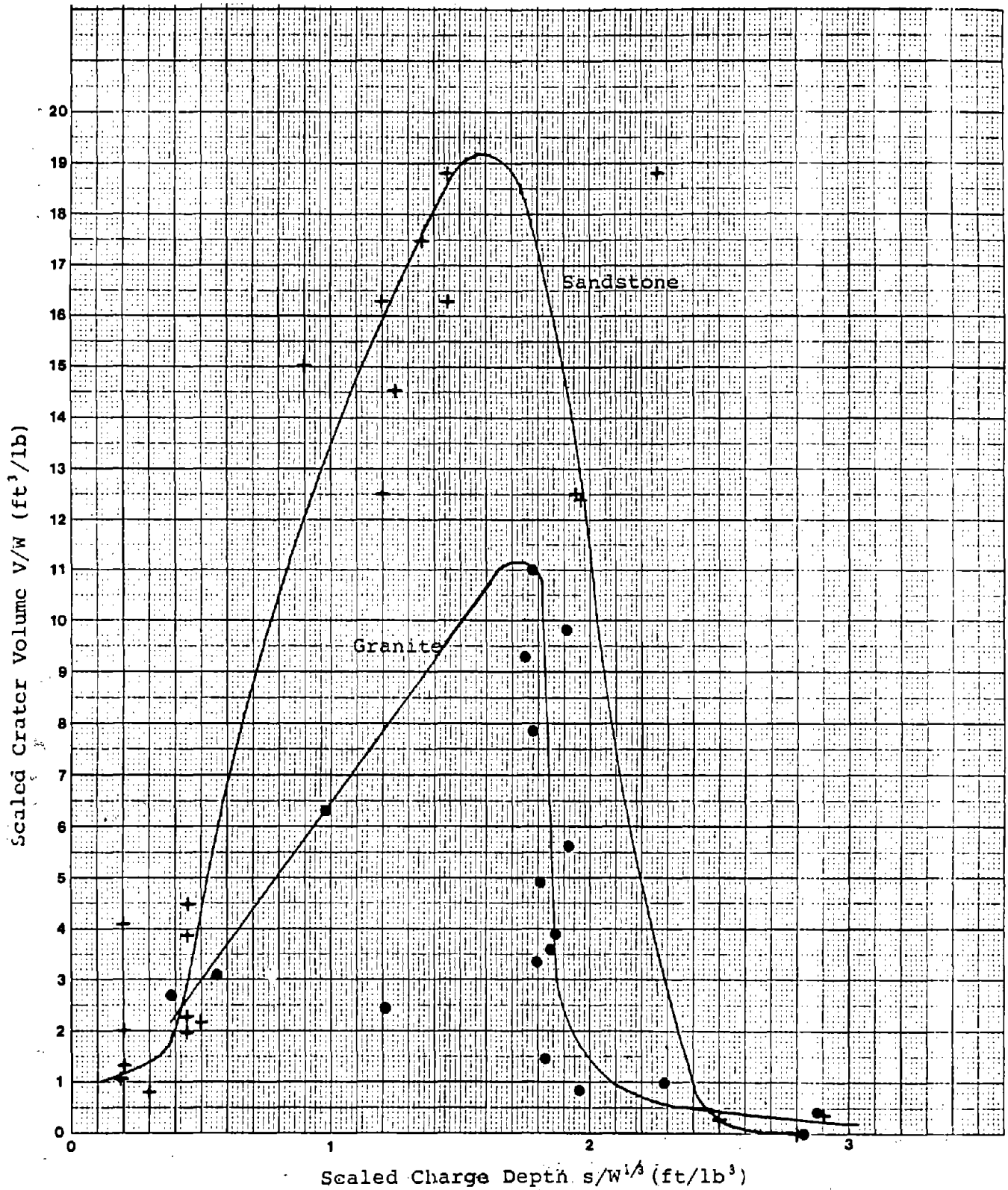


Figure 6: SCALED CRATER VOLUME AS A FUNCTION OF SCALED EXPLOSIVE CHARGE DEPTH

whereas in reality these velocities are decreasing and in the limit of no cratering, become zero.

For shots that are bottom-primed (and most bench shots are) and well-stemmed, the above procedures provide only an upper limit of the initial flyrock velocity because some breakout from the vertical face occurs prior to cratering from the bench top. Obviously, such prior breakout is incompatible with the assumption that the explosive charge is surrounded by a "rigid wall", consequently the computed initial bench top flyrock velocities are overestimates.

In view of the difficulties described above we have also attempted (but only with modest success) to use an alternate empirical approach to estimate initial velocities of flyrock from bench tops. This approach will be discussed in Section 6.4.

6.2 Flyrock Velocities from Bench Tops

We will adapt Equation (12) and the normalization procedure of Section 4.1 to the computation of flyrock velocities from bench tops, with the proviso that c/m in Equation (12) be obtained via Equation (16) rather than Equation (7) which was used for c/m for computing flyrock velocities from vertical faces. Flyrock velocities thus computed are compared with observed velocities in Table 5 for sandstone and in Table 6 for granite, limestone and basalt.

The sandstone data are well represented by the following equation obtained from linear regression analysis:

$$\text{Sandstone: } v_0^2 = 2.266 \times 10^6 (c/m) - 475 \quad (\text{m/sec})^2 \quad (17)$$

(10 data points; $r = 0.999$; normalized to $0.38D = 1750 \text{ m/sec}$)*

* The exact relation between $\sqrt{2E^T}$ and D depends on Γ (see Appendix C). For $\Gamma = 3$, $\sqrt{2E^T} \approx D/3$ and for $\Gamma < 3$, $\sqrt{2E^T} \geq D/3$. For the explosive used to normalize the sandstone data, $\Gamma \approx 2.5$,^{14, 22} and $\sqrt{2E^T} \approx 0.38D$.

<u>Date Source</u>	<u>Explosive</u>	0.38D (km/sec)	Normalized* u_{obs}^2 (m/sec) ²	** c/m x 10 ⁴	Computed [†] u_o^2 (m/sec)
Ref. 16	Gelamite 2	1.75	4099	20.8	4238
"	"	"	753	4.56	558
"	"	"	595	4.56	558
"	"	"	455	3.90	409
"	60 HP gel	2.10 ^{a/}	930	6.08	903
"	"	"	316	4.40	522
"	"	"	161	3.90	409
"	Hercom. B	1.20 ^{a/}	13360	60.8	13302
Ref. 1	ANFO	1.95 ^{b/}	445	3.72	386
"	"	1.98 ^{b/}	228	3.80	386
Ref. 17	ANFO ^{e/}	2.07 ^{b/}	72 ^{c/}	2.7	134
Ref. 18	---	---	≈0 ^{c/d/}	≈1.9	≈-44

* Normalized to 0.38D = 1.75 km/sec (Gelam.2)

**See text for method of computing c/m

† $u^2 = 2.266 \times 10^4 (c/m) - 475$

a/ D/3

b/ 0.44D

c/ Not used in computing slope and intercept.

d/ See footnote g in Table 1.

e/ Hematite waste rock.

Table 5: COMPARISON OF OBSERVED AND COMPUTED FLYROCK VELOCITIES IN SANDSTONE CRATER SHOTS

Data Source	Explosive	$\sqrt{2E}$ (km/sec)	Rock	$s/W^{1/3}$ (ft/lb ^{1/3})	$c/m \times 10^4$	Computed u_0 (m/sec)	Observed u_0 (m/sec)
Ref. 19	ANFO	1.70	Limestone	0.69	13.37 ^{a/}	67 ^{b/}	69 (58-79)
"	"	1.70	"	0.71	13.07 ^{a/}	66 ^{b/}	66
"	"	1.75	"	0.90	9.97 ^{a/}	55.5 ^{b/}	43 (38-47)
"	"	1.75	"	0.21	=58 ^{a/}	=138 ^{b/}	104 (98-109)
"	"	1.79	"	1.00	8.91 ^{a/}	51 ^{b/}	33
"	"	1.98	"	1.5	5.82 ^{a/}	36.5 ^{b/}	≥21 ^{c/}
"	"	1.84	Granite	1.73	5.41	29.5 ^{d/}	45 (37-52)
Ref. 5	Rheolit B	1.67	"	0.48	20.90	60	≥90 ^{e/}
"	"	"	"	0.73	12.89	46	≥73 ^{e/}
"	"	"	"	0.99	9.32	38	≥54 ^{e/}
Ref. 23	TNT	2.10	Basalt	0.14	=65 ^{a/}	136 ^{f/}	≥100
"	"	"	"	"	=65 ^{a/}	127 ^{g/}	≥100

a/ From Figure 3 assuming that the curve for granite also holds for limestone and basalt.

b/ $u_0^2 = [3 \times 10^6 (c/m) - 200] \frac{2E}{(1.88)^2}$; see Eq. 14.

c/ Computed via Eq. 5 from max height of flyrock seen in a still photo. True max height may not have been attained; also rock may have projected at $\theta \neq 90^\circ$.

d/ From c/m and Eq. 13 normalized by $2E/(2.3)^2$.

e/ No stemming

f/ Used Eq. 13

g/ Used Eq. 14

Table 6: COMPARISON OF OBSERVED AND CALCULATED FLYROCK VELOCITIES FOR CRATER SHOTS IN GRANITE, LIMESTONE AND BASALT

Here, as in the bench shots for granite, there may be spalling in the low c/m range (see Table 3).

The few available measurements of crater shot fly velocities in limestone, granite and basalt are compared with computed velocities in Table 6. Agreement between measured and computed values is fair-to-good for limestone and basalt and poor for granite. This is somewhat surprising since we can estimate c/m for granite fairly accurately according to the ascending branch of Figure 6, and we do have well-established constants for the linear relationship between u_0^2 and c/m for granite (Eq. 13), whereas for limestone the constants in Equation (14) are only provisional and we have no data (of the type shown in Figure 6 for granite and sandstone) for estimating c/m for either limestone or basalt. For basalt we also have no constants for the linear u_0^2 and c/m equation. To obtain c/m for limestone and basalt we assumed that both were "granite-like" in their cratering behavior and used the curve for granite in Figure 6 to estimate their c/m. As shown in the last entry in Table 6, use of the granite constants (Eq. 13) or limestone constants (Eq. 14) changes the computed velocity for basalt only slightly.

For granite three of four measured velocities are appreciably higher than the corresponding computed velocities. The three shots for which flyrock velocities were measured were unstemmed. This suggests that lack of stemming may generate greater-than-expected flyrock velocities even though the top of the explosive charge is appreciably below the top of the bench. Obviously, this ad hoc hypothesis needs checking.

6.3 Estimation of Flyrock Range from Bench Tops (Cratering)

Observed and computed flyrock ranges, for flyrock originating from bench tops, are compared in Table 7. The various caveats discussed in Section 5.1 also apply to these shots. A further difficulty is introduced by the uncertainty in estimating c/m for crater shots (see Section 6.1). In some shots it was impossible to determine a priori whether flyrock originated at the vertical face or at the top of the bench. Such shots are listed in both Tables 4 and 7. In general, agreement between observed and computed flyrock ranges for bench top flyrock is surprisingly good.

The results in Table 7 suggest that c/m for "hard" rock (taconite and limestone), for which we have no explicit data, can be obtained from the granite curve of Figure 6. Similarly, the results of Tables 4 and 7 imply that it is permissible to use granite constants (Eq. 13) for taconite, and to use sandstone constants (Eq. 17) for shale as well as the sandstone curve in Figure 6 for estimating c/m for shale.

6.4 Correlation of Bench Top Flyrock Range with c/m or Powder Factors

Observed flyrock ranges from bench tops (as well as flyrock ranges from vertical faces) were presented as a function of c/m in Figure 4 and as a function of powder factors in Figure 5. In the c/m plot, four of eight top flyrock data points fall within the region defined by the computed lines. All four data points outside of this region are below the lowest theoretical line. In the powder factor plot (Figure 5), only one datum point is within the "theoretical" region, two data points are very close to it, and five data points are outside it. Four of these five outside points are well above the top computed line. Thus, as it is for flyrock from vertical faces, correlation between top flyrock range and c/m is appreciably better than the corresponding correlation with powder factors.

Mine	Rock	Bench Height h (feet)	$s/W^{1/3}$ (ft/lb ^{1/3})	$c/m \times 10^{**}$	$\sqrt{2E'}$ (ft/sec)	v_0^2 (ft/sec) ²	L_m (feet)	L'_m (feet)	L_{Obs} (feet)
Reno Construction	Limestone	14	1.65	5.25 ^{a/}	6000	14035	435	450	210
Carbon Limestone	Limestone	50	0.76	12.3 ^{a/}	6480	41555	1290	1338	600
Star Route Quarry	Limestone	36	0.93	10.4 ^{a/}	5600	25966	806	840	850- 1000
Fernsteat Quarry	Limestone	40	~1.0	~9.6 ^{a/}	5750	~25125	~780	~820	450
Mine U	Limestone	70	1.76	5.25 ^{a/}	6580	16881	524	589	~900 ^{b/}
Mine O	Taconite	35	~0.45	~19 ^{c/}	6200 ^{d/}	~44000	~1400	~1430	~1000
Mine M	Taconite	50	1.53	4.76 ^{c/}	6200 ^{d/}	8262	257	300	200- 400
Mine C	Sandstone	60	1.65	3.72	6700	5394	168	~168 ^{e/}	~200
Mine C	Shale	110	3.49	-	6700	~0	~0	~0	0
Mine B	Shale	68	1.72	~3.7 ^{f/}	7020	~5850	~180	~230	~300
Mine I	Shale	44	1.80	~3.7 ^{f/}	6700	~5330	~165	~200	~200

* s = length of stemming column and = weight of explosive column.

** From Figure 6.

a/ From Figure 6 and curve for granite.

b/ Flyrock from vertical face; see Table 4.

c/ From Figure 6 and curve for granite. Equation 13 used to compute v_0^2 .

d/ Slurry explosive; values shown are D/3.

e/ Flyrock landed at about same level as bench top.

f/ From Figure 6 and curve for sandstone.

Table 7: COMPARISON OF OBSERVED AND COMPUTED FLYROCK RANGES FROM BENCH TOPS

6.5 Empirical Correlation Between Velocities of Bench Top Flyrock and Depth of Charge Burial

From preceding discussions it is evident that use of the Gurney approach to compute flyrock range for bench top flyrock is beset by many uncertainties and moreover requires experimental data (Figure 6) for the estimation of c/m . Consequently, we have tried a purely empirical correlation of flyrock velocity and scaled depth of burial of the explosive. Figure 7 is a log-log plot of observed flyrock velocity (mostly measured but some calculated from measured flyrock range with θ assumed to be 45°) as a function of $s/W^{1/3}$ for granite, limestone and sandstone. The observed velocities were normalized by the procedure described in Section 4.1. The distance s (depth of burial) is from the borehole collar to the top of the explosive column.

Examination of Figure 7 reveals that for $s/W^{1/3} < 1.5 \text{ ft/lb}^{1/3}$ the plots for granite and sandstone appear to be linear. The limestone data in this range vary appreciably but appear to fall mostly within the region defined by the granite and sandstone lines. Note that for a given $s/W^{1/3}$ the flyrock velocity for granite (and consequently flyrock range) is appreciably greater than the flyrock velocity for sandstone. For $s/W^{1/3} > 1.5 \text{ ft/lb}^{1/3}$ there still appears to be a linear relation between $\log v_o$ and $\log s/W^{1/3}$ but the slope of this line is much steeper than the corresponding slope of the lines in the region of $s/W^{1/3} < 1.5$. Such a change in slope is not unexpected since v_o rapidly approaches zero as $s/W^{1/3}$ exceeds 2 to 3 $\text{ft/lb}^{1/3}$. Included in Figure 7 are spall velocities, computed via Equation (15), for $s/W^{1/3}$ ranges where spalling may predominate. The slopes of these computed spall lines (broken lines in Figure 7) appear to be steeper than the "eye-ball" line (heavy line in Figure 7) through the data for $s/W^{1/3} > 1.5$.

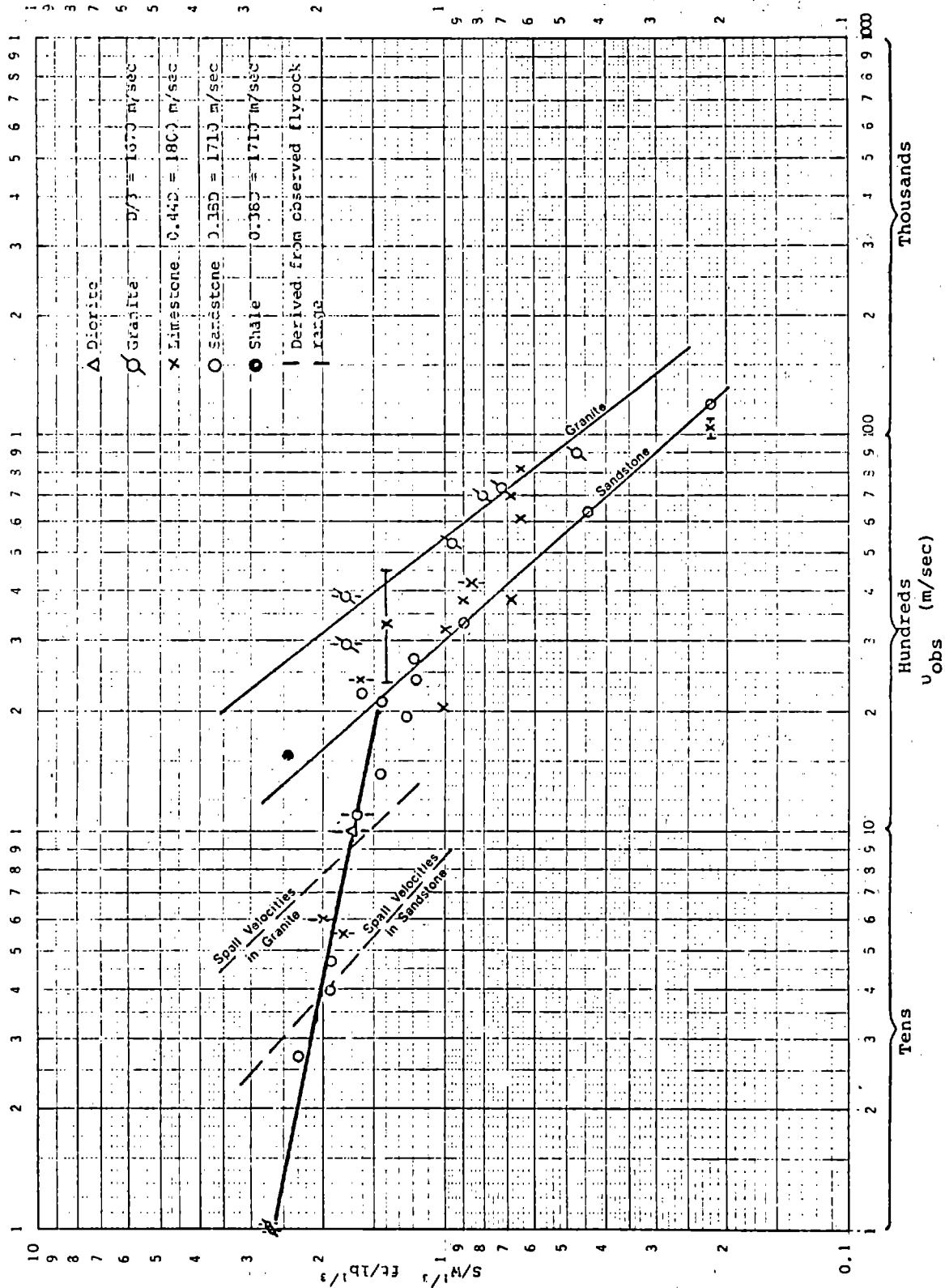


Figure 7: EMPIRICAL CORRELATION OF BENCH-TOP FLYROCK WITH SCALED DEPTH OF CHARGE BURIAL

Flyrock ranges, for granite and sandstone, based on the empirical correlation of Figure 7 are compared with flyrock ranges computed from the Gurney model in Table 8 for $s/W^{1/3} \leq 1.75 \text{ ft/lb}^{1/3}$. Agreement between these two methods of estimating flyrock range for bench top flyrock is fairly good. The maximum difference between these two sets of estimates is about 27%. For $s/W^{1/3} > 1.75 \text{ ft/lb}^{1/3}$ we have no means of estimating c/m (see Figure 6 and discussion in Section 6.1). Thus, no comparison can be made between the empirical and Gurney methods. In any case, the flyrock range under these conditions ($s/W^{1/3} > 1.75$) is expected to be small.

Rock	Assumed $s/W^{1/3}$ (ft/lb ^{1/3})	u_o^* (m/sec)	L_m^* (m)	$c/m \times 10^4$ ***	u_o^2 (m/sec)	u_o (m/sec)	L_m^{**} (m)
Granite	1.75	35	125	5.46	1320 ^{a/}	36	135
Granite	1.5	39	155	6.06	1529 ^{a/}	39	156
Granite	1.0	54	297	9.32	2666 ^{a/}	52	272
Granite	0.5	94	900	21.6	6460 ^{a/}	83	708
Sandstone	1.6	20	41	3.72	368 ^{b/}	19	38
Sandstone	1.3	24	59	4.20	477 ^{b/}	22	49
Sandstone	1.0	30	92	5.29	724 ^{b/}	27	74
Sandstone	0.7	42	180	8.21	1385 ^{b/}	37	141
Sandstone	0.5	56	320	17.0	3377 ^{b/}	58	344

* From Figure 7

** From Equation (2)

*** From Figure 6

a/ From Equation (13)

b/ From Equation (17)

Table 8: COMPARISON OF EMPIRICAL AND GURNEY-MODEL FLYROCK RANGES FOR BENCH TOP FLYROCK

7.0 "WILD" FLYROCK

Wild flyrock may be defined as flyrock that travels much further than flyrock that is normally encountered in any given blasting operation or further than estimated by existing rules of thumb (see Section 8). Table 9 shows a comparison between computed flyrock ranges and observed flyrock ranges for shots in which the latter is much larger than the former. Obviously, wild shots can be extremely dangerous. Thus, every effort should be made to determine what causes a shot to become wild. Unfortunately, information on shot conditions that obtained for these wild shots is scarce and insufficiently detailed. For four of the 10 shots shown in Table 9 the MESA accident investigation reports gave essentially no details about shot conditions. Possibly four or five of the 10 shots had the explosive column too high in the borehole. One or two wild shots have been attributed to fissures.

There is certainly no doubt that a borehole loaded almost to the collar will throw rock over a wide distance. This type of overload must be avoided. If part of the borehole caves in just prior to loading or during loading, the explosive column, if unchecked, can also come close to the collar. Similarly, if some of the explosive cartridges (ANFO) float up in wet holes wild flyrock may be generated. Clearly it is very important to monitor the distances between the top of the charge and the hole collar before the hole is stemmed. If at all possible, $s/W^{1/3}$ should be kept greater than $2 \text{ ft/lb}^{1/3}$. This will keep bench top flyrock down to a minimum.

Other causes for wild flyrock are much more difficult to establish. Obviously, a sufficient burden must be maintained for every hole near a free face. This is easier said than done. Vertical faces are usually irregular and a small caved-in portion of the face may result in a much smaller burden in the region of the cave-in than the average burden. Potentially even more hazardous are undetected internal cave-ins or fissures. They may reduce burdens drastically. Preliminary results (see data marked with b/ in Table 2) indicate that considerable decoupling of

Mine	Rock	Computed L_m (feet)		L_{obs} (feet)	Powder Factor lbs/yd ³	Possible Cause
		Bench Top	Vertical Face			
Conklin Quarry	Limestone	~430	~230	1200	0.45	Overloaded holes (?)
Sibley Quarry	Limestone	small a/	~125	475	0.9	Undetermined
Roberta Quarry	Limestone	~150	~135	1600	~1.7	Undetermined
Falling Springs Quarry	Limestone	~790	~270	2000	0.7 max.	Fissures; also mar- sinal stemming
Okalona Quarry	Limestone	a/	a/	1600	a/	Overloaded holes
Oglesby Quarry	Limestone	a/	a/	2500	a/	Undetermined
Latah Quarry	Trap Rock	~0 c/	30-120 ^{b/}	330	0.68	Undetermined ^{d/}
Mine O	Taconite	~1430 avg.	~300 max.	4500	1.2 avg.	Insufficient stemming
Berkely Pit	Porphyry	~0 c/	a/	840	a/	Some holes may have partially caved in; consequently explo- sive load could have risen much higher than planned.
Mine A	Sandstone	~235	~20	~800	0.53	Fissures

a/ Insufficient information to compute.

b/ Lower value computed with granite constants; higher value computed with limestone constants.

c/ According to shot conditions given in the report.

d/ Flyrock must have originated at bench top since observed flight time is much too long for flyrock from vertical face.

Table 9: "WILD" FLYROCK

charge and burden does not alter flyrock velocity. This suggests that to a first approximation the flyrock velocity produced by a given explosive load for boreholes with and without intersecting internal cavities will vary inversely as the minimum burden (rock thickness) of the respective conditions. For example, if the minimum burden for a hole in uncavitated rock is b and that for cavitated rock in the region of the intersecting cavity is $b/2$, the expected flyrock velocity of the latter is about twice the former, and flyrock range of the latter is about four times the former.

Fissures extending close to the free face may produce an additional dangerous effect. Loose rocks within such fissures may be shot out as "cannon-balls"; i.e., the fissure acts as a gun barrel and permits a much longer acceleration time of the loose rock than is normally encountered in open pit blasting. Incidentally, Swedish studies⁵ indicate that loose rocks on the surface of a crater shot achieve a fly velocity that is essentially equivalent to that obtained in a similar crater shot without loose rocks on its surface.

In Table 9 we included powder factors whenever such information was available. Note that there is no correlation between powder factor and flyrock range. In view of the discussion above this is to be expected. Certainly powder factors provide no information about the presence of cavities or fissures. Since powder factors are computed from average loads per hole they provide little or no warning about a few holes that may be overloaded; i.e., holes in which the charge comes close to the borehole collar.

Incorrect or inaccurate delays between holes can conceivably generate wild flyrock. The possible effects of incorrect timing were discussed in Section 3.2.3.

8.0 ESTIMATION OF FLYROCK RANGE FOR FIELD USE

The results and conclusions of the preceding sections are of limited value unless they can be adapted for field use. Consequently a series of simple charts have been developed which give flyrock range as a function of shot conditions. These charts as well as direction for their use are presented in Appendix D. If deemed suitable, the contents of Appendix D can be distributed to field personnel.

In this section we will briefly summarize prior attempts at estimating flyrock range and present the rationale for the charts in Appendix D.

8.1 Prior Attempts at Estimating Flyrock Range

There appears to be a rule-of-thumb of unknown origin and rationale which states that flyrock range is three times the bench height. According to the data in Table 10 this rule-of-thumb is highly unreliable since in about two-thirds of the comparisons shown (lower grouping in Table 10) it predicts incorrect flyrock ranges. Moreover all but one of these false predictions are underestimates and some are gross underestimates.

For bench top flyrock a comparison between rule-of-thumb and observed flyrock range is even worse than that shown in Table 10 for vertical face flyrock. Only two of 10 comparisons are reasonably close. Again, the rule-of-thumb generally grossly underestimates flyrock range.

Ash²⁴ suggests that the ratio of stemming height to burden (s/b) be maintained larger than 2/3 to prevent bench top flyrock. He also suggests that, on the average, b/d for efficient blasting should be about 30 (but the range here is wide: 14 for "weak" explosives in hard material and 49 for "strong" explosives in soft material). The maximum load per

<u>Mine</u>	<u>Rock</u>	<u>Bench Height=h (ft)</u>	<u>Observed Flyrock Range</u>	<u>3h (ft)</u>
Mine D	Sandstone	20	~50	60
Mine J	Porphyry	40	~100	120
Mine P	Porphyry	25	<50	75
Mine K	Diorite	50	~100	150
Mine V	Limestone	117	~350	351
Mine X	Diabase	80	<200	240
Annapolis Quarry	Granite	52	200-400	150
Mine H	Shale	40	~400	120
Mine C	Shale	110	~20	330
Mine B	Shale	68	~300	204
Nolin Coal	Shale	27	210	81
Roberson Coal	Shale	30	400	120
Mine W	Limestone	50	~300	150
Mine U	Limestone	60	~900	180
Mine R	Dolomite	60	~250	180

Table 10: COMPARISON OF RULE OF THUMB AND OBSERVED FLYROCK RANGES FOR FLYROCK FROM "VERTICAL" FACES

borehole, according to Eq. 7.3-18 of Ash's article is given by

$$W_{\max} = \frac{\rho_c \pi d^2}{4} (3b-s) = 1.81 \rho_c d^2 b, \quad \text{if } s=0.7b.$$

Then,

$$s/W^{1/3} = 0.7b / (1.81 \rho_c)^{1/3} d^{2/3} b^{1/3} = (0.574 / \rho_c^{1/3}) (b/d)^{2/3},$$

and with $b/d = 30$ (according to Ash) and $\rho_c = 53 \text{ lb/ft}^3$ (for ANFO),

$$s/W^{1/3} = 1.48 \text{ ft/lb}^{1/3}$$

According to the plots in Figure 7 this value of $s/W^{1/3}$ can still lead to far-ranging bench top flyrock at least for shots in granite and possibly also in limestone (see Table 7).

Still another attempt to estimate flyrock range was published by Lundborg, et. al.²⁵ Their study was concerned primarily with crater shots. Based on conservation of momentum, scaling laws for spherical explosive charges, and ballistic trajectories they obtained a relation between flyrock range and borehole diameter. The constants in this relation were obtained empirically and their final result for maximum flyrock range is

$$L_m = 853d^{2/3} \tag{18}$$

where L_m is in feet and d is in inches.

Unfortunately, even a cursory comparison of the flyrock range computed by this formula with observed bench top flyrock range (Table 7) shows that this formula grossly overestimates flyrock range. This is illustrated in the following tabulation:

<u>Mine</u>	<u>d</u> <u>(inches)</u>	<u>L_{obs}</u> <u>(ft)</u>	<u>853d^{2/3}</u> <u>(ft)</u>
Fernsteat Quarry	3.5	450	1966
Mine U	6.75	900	3047
Mine C	12	~0	4471
Mine I	9	~200	3690
Star Route Quarry	3	850-1000	1774

It appears that the empirical constants of Equation (18) were mostly obtained from measurements of flyrock range of unstemmed shots, and from flyrock ranges computed from ballistic trajectories based on velocity measurements of flyrock from small-scale crater shots. If the fly in these small-scale shots was mostly vertical ($\theta=90^\circ$), the horizontal flyrock range would be much less than that computed from these velocities for $\theta = 45^\circ$. Intuitively one would expect that unstemmed shots propel flyrock further than stemmed shots. Consequently the empirical constants thus obtained may be too large for most production blasts.

Equation (18) does, however, appear to give the right order of magnitude of the flyrock range of about half the "wild" shots listed in Table 9. This is shown in the following tabulation:

<u>Mine</u>	<u>d</u> <u>(inches)</u>	<u>L_{obs}</u> <u>(ft)</u>	<u>853d^{2/3}</u> <u>(ft)</u>
Okalona Quarry	2.5	1600	1571
Roberta Quarry	3	1600	1774
Conklin Quarry	3.5	1200	1996
Mine O	9-15	4500	3690-5188

Lundborg, et. al.²⁵ state that the flyrock range from vertical faces is roughly one-sixth that of flyrock range of similar shots that break out at the bench tops (crater). Although their formula for flyrock range from vertical faces

generally overestimates the flyrock range in production blasting, their qualitative conclusion agrees with our conclusion that most far-ranging flyrock comes from bench tops and not from vertical free faces (see Section 5.1).

8.2 Rationale for Field Use Charts for Flyrock From Vertical Faces

As shown in the previous sections, the shot variables that control flyrock are: rock type, c/m , D the detonation velocity of the explosive charge for the conditions of the shot, and to a lesser degree face height h or height of the explosive column, l .

Equation (7) can be transformed into:

$$c/m = \frac{\rho_c \pi d^2}{4 \rho_m b^2} \quad \text{if } \alpha/2 \text{ is assumed to be } 45^\circ. \quad (19)$$

D , for a given explosive, can be expressed as a function of d . Thus, L_m , the maximum flyrock range for a given rock, shot with a given explosive, for flyrock striking at the same elevation as its original elevation in the rock face, can be completely defined in terms of the borehole diameter d and the minimum burden to the free face b .

The explosive used in most open pit blasting is ANFO. Consequently, all our results about to be presented are for ANFO at a loading density (ρ_c) of 0.85 g/cm^3 . The following relation between d and $0.44D$ was used.

<u>d</u> <u>(Inches)</u>	<u>0.44D</u> <u>(Ft./Sec.)</u>
2	4900
3	5300
4	5900
6	6450
9	6700
12	6800
15	6850

These values were obtained from an Eyring-type plot of D vs. 1/d of ANFO detonation velocities from several published sources.

For granite, a combination of Equations (2), (13), and (19) gives the following expression for L_m as a function of d/b:

$$L_m = 0.334 \left[8.95 \times 10^5 (d/b)^2 - 584 \right] (0.44D/7544)^2 \quad (\text{ft}) \quad (20)$$

The bracketed squared term on the far right transforms the normalized L_m values of Equation (13) to L_m for the actual shot conditions. The density of granite, ρ_m , was taken to be 2.6 g/cm³.

Analogously, for sandstone (substituting Eq. (17) for Eq. (13)):

$$L_m = 0.334 \left[6.86 \times 10^5 (d/b)^2 - 475 \right] (0.44D/5740)^2 \quad (\text{ft}) \quad (21)$$

The density of sandstone was taken to be 2.2 g/cm³.

For limestone (using Equation 14) provisional values for L_m are:

$$L_m = 0.334 \left[7.42 \times 10^5 - 200 \right] (0.44D/5490)^2 \quad (\text{ft}) \quad (22)$$

The density of limestone was taken to be 2.7 g/cm³.

In the field, borehole diameter, d , is usually fixed by the availability of drilling equipment and burden, b , can usually be adjusted to obtain the desired blast results. Thus it is logical to develop charts for field use that relate L_m to b for various fixed values of d . A series of such curves for granite is shown in Figure 8 (more curves are given in Appendix D). Note that on a semi-log scale the relation between L_m and b is linear over the range examined for $3" \leq d \leq 6"$. For $d > 6"$ there appears to be a break in the linear plots at $L_m < 100$ ft (the broken lines in Figure 8).

In blasting hard rock or blasting under wet conditions, slurry explosives are often used instead of ANFO. Thus it is desirable to estimate the effect that substitution of slurries for ANFO will have on the plots in Figure 8. Unfortunately there are many commercial slurry explosives available and their explosive characteristics can vary appreciably. Consequently, no unique explosive properties can be assigned to a "generic" slurry explosive. In general slurries are denser than ANFO and have a higher detonation velocity than ANFO under comparable conditions. However, some scanty data²² suggest that $\sqrt{2E^T} \approx D/3$ for slurries whereas $\sqrt{2E^T} \approx 0.44D$ for ANFO. Thus, as far as $\sqrt{2E^T}$ is concerned, the higher D of slurries is counterbalanced by the higher numerical factor of ANFO, but the higher density of slurries will result in a larger c/m than that for ANFO at any given borehole diameter. On the basis of Equations (13), (14), or (17), we can anticipate that the flyrock range of any diameter borehole loaded with slurry will be greater than the flyrock range of the same borehole loaded with ANFO.

In Figure 8 we have plotted L_m vs. b curves for a "low" density and a "high" density slurry. The low density slurry is Hercules Gel Power 0 at 1.15 g/cc. The detonation velocities for this slurry were interpolated from data given in the manufacturer's trade literature. The high density slurry is DuPont's Pourvex Extra at 1.33 g/cc. Trade literature gives only a single value of $D = 4900$ m/sec for $d = 5"$ (under confinement).

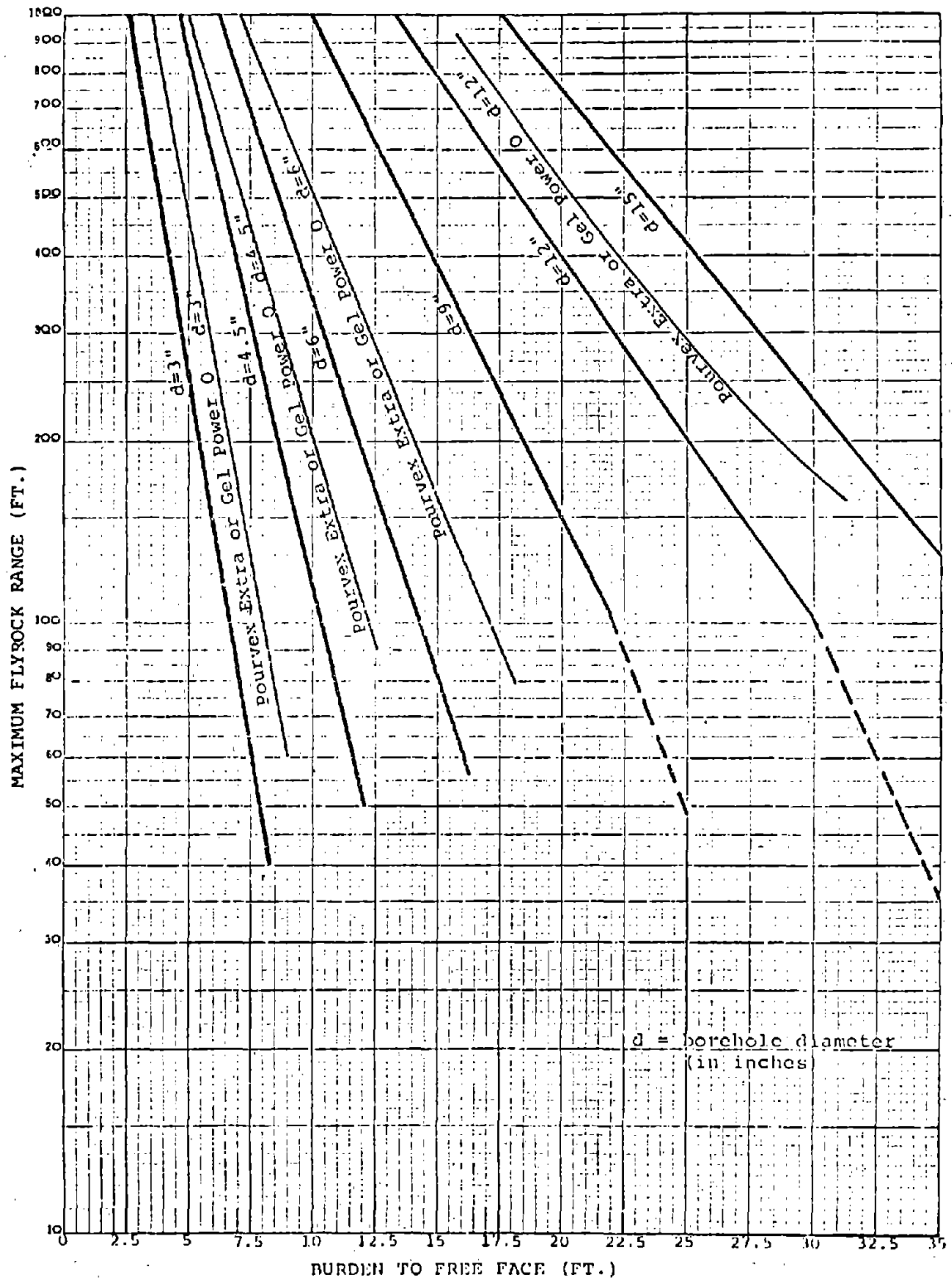


Figure 8: FLYROCK RANGE FROM VERTICAL GRANITE FACES SHOT WITH ANFO OR SLURRY EXPLOSIVES

Comparison of the ANFO and slurry plots suggests that over the range of borehole diameters examined the ratio of flyrock range $(L_m)_{\text{slurry}} \div (L_m)_{\text{ANFO}} = 1.5$.

The flyrock ranges L_m in Figure 8 are the horizontal distances from the free face to a plane at the same vertical elevation as the original position of the chunk of rock in the free face. If "floor level" of the pit is appreciably below this elevation, flyrock will travel further than L_m . This greater range, L'_m , is defined by Equation (3). A chart for converting L_m to L'_m is included in Appendix D.

8.3 Rationale for Field Use Charts for Flyrock from Bench Tops

These data are more difficult to present in simple form than data for flyrock from vertical faces. Also, the bench top data are less reliable than the vertical face data. Because the Gurney method of calculating flyrock ranges for crater shots involves too many variables to be combined into a single chart, we have chosen to use an empirical approach. Measured flyrock velocities for sandstone, limestone and granite were plotted on log-log paper vs. $s/W^{1/3}$ in Figure 7. We have no theoretical justification for the apparent linearity of these plots. Since the v_o of Figure 7 is related to L_m by Equation (2), one can construct L_m vs. $s/W^{1/3}$ plots. Such plots are given for ANFO loaded shots in granite and in sandstone in Figure 8-D of Appendix D. It should be recalled that s is the distance from borehole collar to top of the explosive column. The borehole diameters chosen for the plots cover the usual production blasting range. Note that the flyrock range for granite shots appears to be roughly three times greater than the flyrock range for shots in sandstone. Since limestone flyrock velocities in Figure 7 lie between those of sandstone and granite, it is to be expected that limestone flyrock ranges will also fall between the ranges for sandstone and granite. In the region of $s/W^{1/3}$ of 1.5 to 2 ft/lb^{1/3} there

is a break in v_o vs. $s/w^{1/3}$ plot (Figure 7). Consequently the plots for sandstone in Figure 8-D were terminated at $s/w^{1/3} = 1.5 \text{ ft/lb}^{1/3}$. Similarly a break in the granite plot of Figure 7 occurs in the region of $s/w^{1/3} = 2$ to $2.75 \text{ ft/lb}^{1/3}$. Consequently the granite plots in Figure 8-D were terminated at $s/w^{1/3} = 2 \text{ ft/lb}^{1/3}$. Below these termination regions L_m is expected to decrease rapidly.

9.0 RECOMMENDATION FOR ADDITIONAL FLYROCK STUDIES

It has been shown that an adaptation of the Gurney method, developed in this study, can predict maximum flyrock range over a wide spectrum of shot conditions. However, there are a number of assumptions used in this computational method that still remain unverified because the necessary experimental data for verification do not exist. Similarly, some of the required constants for the computation are not known to the desired degree of accuracy again because the required experimental data are lacking. Thus, to complete our understanding of the relation between shot conditions and flyrock range, answers must be provided to several general and several specific questions.

The general questions that need to be answered are: (a) does the Gurney method, developed for a single hole model, require modification to adapt it to multiple hole shooting? At present we have found indirect evidence to answer this question in the negative, but it would be most desirable to obtain actual data for shots under comparable conditions in which one set of data are for single hole shots and a comparative set of data are for multiple hole shots; (b) can mistiming of shot delays in a multiple hole round drastically affect flyrock range? For most well-designed blasts, and in the absence of utterly gross mistiming, our present understanding of the problem leads us to answer this question in the negative. However, we may be in the minority with our point of view. The proper way to settle this question is by appropriate experiments; (c) what causes "wild" flyrock? Is it primarily improper shot design or is it some undetected fault in the rock strata? There is no doubt that improper shot design in the form of overloaded holes (too high a rise of the explosive column or too little burden) will produce wild flyrock. Whether mistiming can do this is questionable. In any event one can purposely alter shot conditions to determine if these alterations (other than overloading) result in wild flyrock. The effects of faults in the rock are much more difficult to assess. Studies with transparent small-scale models may provide some guidance, but like most scaled-down

model tests of rock blasting they are expected to be of limited value. A more useful approach is to produce artificial faults in reasonably homogenous rock through a judicious combination of drilling and small-scale blasting. Shots in which artificial faults have been introduced between the borehole and the free face can then be compared to similar shots with no artificial faults in the rock.

There appears to be little hope of finding much useful data on wild shots in accident reports. Fortunately wild shots are not too frequent. Thus, the data base at best will be small. Further problems arise from the fact that most of the accident reports of wild shots are grossly lacking in the necessary details for establishing the cause of these wild shots. Clearly an experimental approach is required to obtain an understanding of the factors that contribute to the production of wild flyrock. Though wild shots are infrequent, their hazard potential is great. Consequently the elimination of wild flyrock is a most worthwhile improvement in blasting safety.

The specific questions that need to be answered deal primarily with flyrock from limestone and shale. These two rock types are probably shot much more frequently in the U.S. than all other rock types combined. The questions are: (a) what is the relationship between $s/W^{1/3}$ and V/W for crater shots in limestone or in shale? In the present study it was assumed that limestone is "granite-like" and shale is "sandstone-like". These assumptions need verification via actual crater shots. These shots could also be used to check the validity of our assumption that elongated explosive loads behave like concentrated loads if s is taken to be the distance from borehole collar to the top of the elongated load rather than the distance to the center of mass of a concentrated load (b) preliminary data on crater shots in granite suggest that observed flyrock ranges from such shots are greater than the computed ranges. Is this a valid conclusion? Here, complete analysis of the Martin-Marietta data⁹ may provide the answer; (d) how valid is the assumption that $\sqrt{2E^T} \approx D/3$ for slurry explosives? Some data justifying this assumption is given in Reference 22, but additional measurements would be desirable.

In summary, certain aspects of the correlation between flyrock range and shot conditions, still unanswered by the present study, can be clarified by:

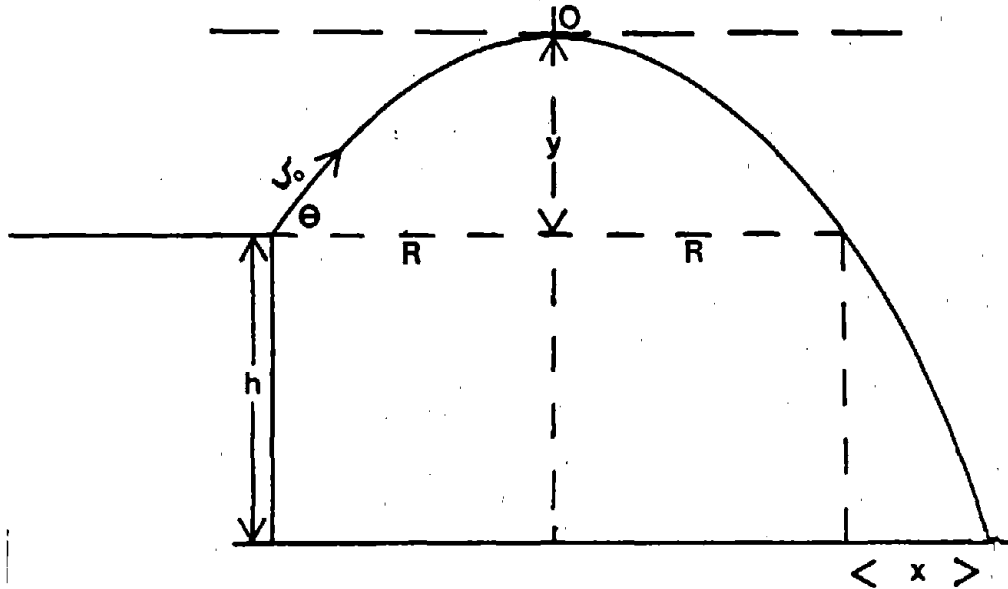
- examination and analysis of the flyrock data of the on-going Martin-Marietta studies;
- an experimental program primarily directed to obtain a better understanding of crater shots which appear to be the kind of shots that can throw flyrock far and in unexpected directions.

10. REFERENCES

1. Roth, J., et. al., "Evaluation of Surface Mine Blasting Procedures," Management Science Associates, Bureau of Mines Contract No. J0366017 (1977).
2. Gurney, R. N., Ballistics Research Laboratory Report No. 405 (1943).
3. Roth, J., SRI Laboratory Technical Report No. 001.71 (1971).
4. Noren, C. H., "Colorado School of Mines Quarterly," 51, 222 (1956).
5. Ladegaard-Pederson, A., and Persson, A., "Svedefo Report," DS 1973:13 (1973).
6. Anonymous, DuPont Blaster's Handbook, 175th Anniversary Edition, p. 242 (1978).
7. Ibid, p. 308.
8. Cook, M. A., The Science of Industrial Explosives, Chapter 10 (1974).
9. Nicholls, H. R., and Hooker, V. E., "RI 6693", p. 43 (1965).
10. Nicholls, H. R. and Duvall, W. I., "RI 6806", pp. 12-14, (1966).
11. Nicholls, op. cit., p. 43 (1965).
12. Noren, C. H., and Porter, D. D., Proceedings 3rd Congress of Int. Soc. Rock Mech., Vol. 2B, 1371 (1974).
13. Langefors, U., and Kihlstrom, B., Rock Blasting, pp. 46-49, Almquist and Wiksell, Stockholm (1963) (Quotation).
14. Duvall, W. I., and Atchison, T. C., "RI 5356", pp. 34-35 (1957).
15. Bergmann, O. R., et. al., "Int. J. Rock Mech. Min. and Geomech.," Abstract, Vol. 10, 585 (1973).
16. Petkof, B., et. al., "RI 5849," p. 9 (1961).
17. Chung, S., et. al., "Preprint 10th Canadian Symposium on Rock Mechanics," (1975), and Chung, S., "Report from CIL Explosives Research Lab, September 16, 1975.
18. Langefors, U., op. cit., p. 70 (1963).

19. Montenyohl, V., Private communication, Martin-Marietta Labs, Baltimore (1978).
20. Blair, B. E., "RI 5584," (1960).
21. Shimomura, Y., and Yamaguchi, V., J. Industr. Explosives Soc. (Japan), Vol. 32, No. 1, p. 49 (1971).
22. Finger, M., et. al., "Proc. 6th Detonation Symposium," 729, (1976).
23. Henny, R. W., and Carlson, R. H., "Ann. N. Y. Acad. Sci.," 152, 417 (1968).
24. Ash, R. L., Surface Mining (E. G. Pfeleider, Editor), Chapter 7.3, pp. 373-397 (1968).
25. Lundborg, N. et. al., Engineering and Mining Journal, 95 (May 1975).
26. Persson, P. A., et. al., "Proc. 2nd Congress of the International Society for Rock Mechanics," 5-3, p. 1 (1970).
27. Anderson, G. D., SRI Internal Report 007-59 (1959).

APPENDIX A
ELEVATION CORRECTION FOR BALLISTIC TRAJECTORIES



Parabolic trajectory starts at velocity u_0 , angle θ and elevation h_0 . Place coordinate origin at O , then:

$$y = cR^2 \quad \text{and} \quad y + h = c(R+x)^2$$

or dividing:

$$1 + \frac{h}{y} = 1 + \frac{2x}{R} + \left(\frac{x}{R}\right)^2 \quad \text{and} \quad \left(\frac{x}{R}\right)^2 + \frac{2x}{R} - \frac{h}{y} = 0$$

or

$$x^2 + 2xR - \frac{h}{y}R^2 = 0$$

and

$$x = \frac{-2R + \sqrt{4R^2 + 4hR^2/y}}{2} = -R + R\sqrt{1+h/y} = R(\sqrt{1+h/y} - 1)$$

but from Eqs. (1) and (5), $y = R/2$ (y is called h_m in Eq. 5),
therefore

$$x = R\sqrt{1 + 2h/R} - 1 = (L_m/2) (\sqrt{1 + 4h/L_m} - 1)$$

since $R = L_m/2$.

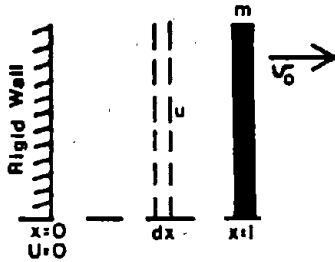
Finally,

$$L'_m = L_m + x = (L_m/2) (\sqrt{1 + 4h/L_m} + 1).$$

APPENDIX B

DERIVATION OF THE GURNEY EQUATION FOR A PLATE DRIVEN BY A
HEAD-ON DETONATION ORIGINATING AT A RIGID WALL

The sketch below represents a cross-sectional view of the system at some time after initiation.



m = mass/unit area of propelled material
 c = mass/unit area of explosive
 U = expansion velocity of product gases at $x = 0$

The Gurney assumptions are:

- a. Product gas density, ρ , is uniform at any given time.
- b. Velocity distribution u of the expanding product gases is linear; thus an element of gas, dx , has a mass/unit area of ρdx and the entire product gas mass is $\rho \int_0^l dx = \rho l$

1. Conservation of mass (and assumption a):

$$c = \rho l \quad (B-1)$$

2. Kinetic energy of plate = $\frac{1}{2} m u_0^2$ (B-2)

3. Kinetic energy of gas = $\frac{1}{2} \int_0^l \rho u^2(x) dx$, but from assumption b $u(x) = u_0 \left(\frac{x}{l}\right)$, therefore

$$\frac{1}{2} \int_0^l \rho \frac{u_0^2 x^2}{l^2} dx = \frac{\rho u_0^2}{2l^2} \int_0^l x^2 dx = \frac{\rho l u_0^2}{6}$$

Substitution from Equation (B-1) gives

$$\text{K.E. gas} = \frac{c}{6} u_o^2 \quad (\text{B-3})$$

4. If all the explosive energy E goes into K.E. of gas and plate, then from conservation of energy:

$$cE = \frac{1}{2} m u_o^2 + \frac{c}{6} u_o^2 \quad (\text{B-4})$$

or

$$2E = \left(\frac{m}{c} + \frac{1}{3}\right) u_o^2 \quad (\text{B-5})$$

and

$$u_o = \sqrt{2E \left(\frac{m}{c} + \frac{1}{3}\right)^{-1/2}} \quad (\text{B-6})$$

$$\text{If } m/c \gg 1/3 \quad u_o \approx \sqrt{2E} \sqrt{c/m} \quad (\text{B-7})$$

APPENDIX C

CORRELATION OF THE GURNEY CONSTANT WITH DETONATION VELOCITY

The writer showed³ for head-on detonations the Gurney constant $\sqrt{2E}$ can be expressed as

$$\sqrt{2E} = \frac{0.605}{\Gamma-1} D \quad (C-1)$$

where detonation product gases are assumed to obey a polytropic equation of state with a coefficient Γ such that

$$P_j = \frac{\rho_o D^2}{\Gamma+1}$$

where P_j is the detonation pressure, ρ_o is the initial density of the explosive and D is the detonation velocity. For tangential detonations the Gurney constant $\sqrt{2E'}$ is given by

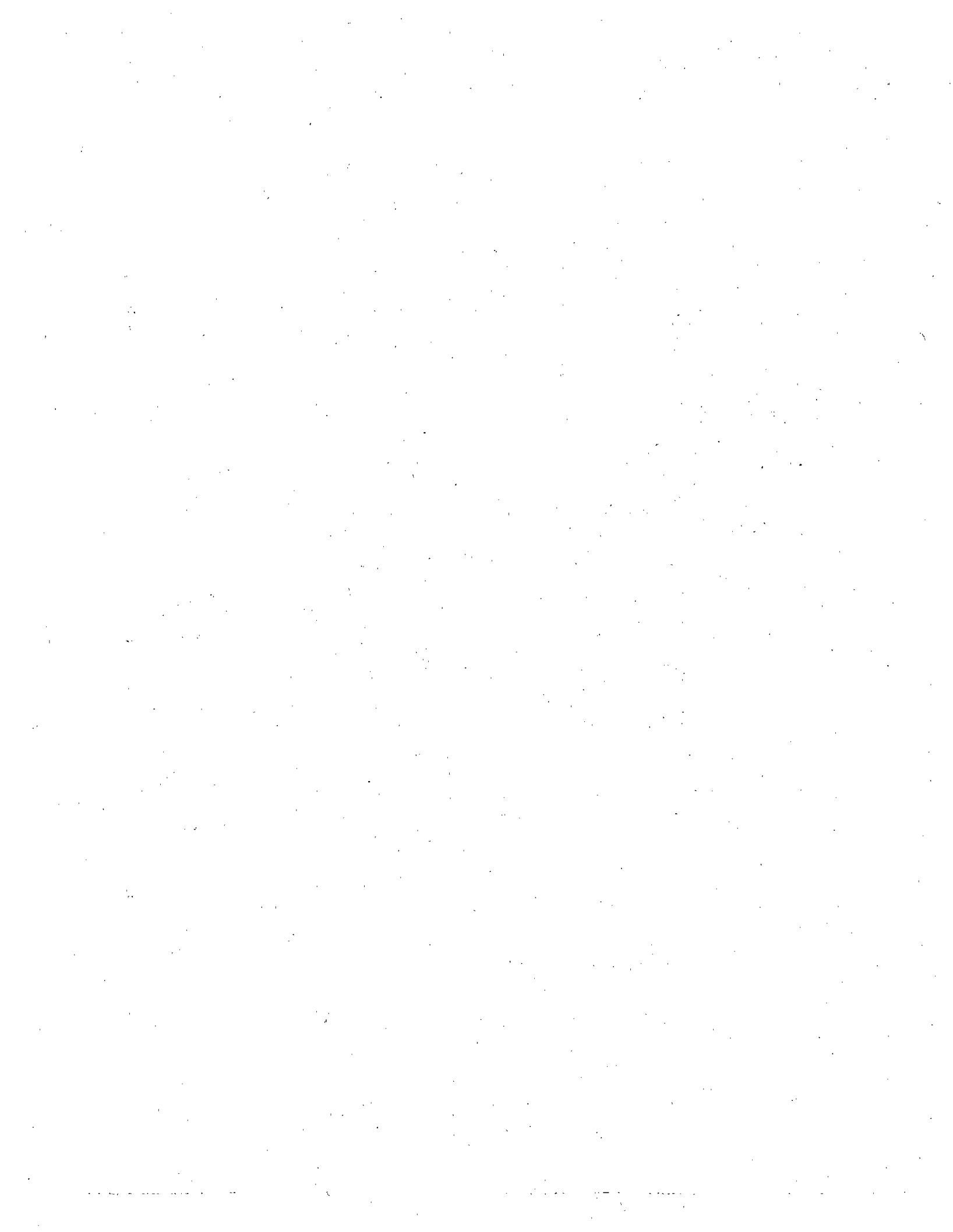
$$\sqrt{2E'} = 0.95\sqrt{2E} \quad (C-2)$$

For many explosives $\Gamma \approx 2.8$. Then, according to Equations (C-1) and (C-2)

$$\sqrt{2E'} \approx D/3 \quad (C-3)$$

However, for ANFO, P_j and D data obtained at Lawrence Livermore Laboratories²² give $\Gamma = 2.3$. Consequently, for ANFO

$$\sqrt{2E''} \approx 0.44D \quad (C-5)$$



APPENDIX D
CHARTS FOR ESTIMATING MAXIMUM FLYROCK RANGE

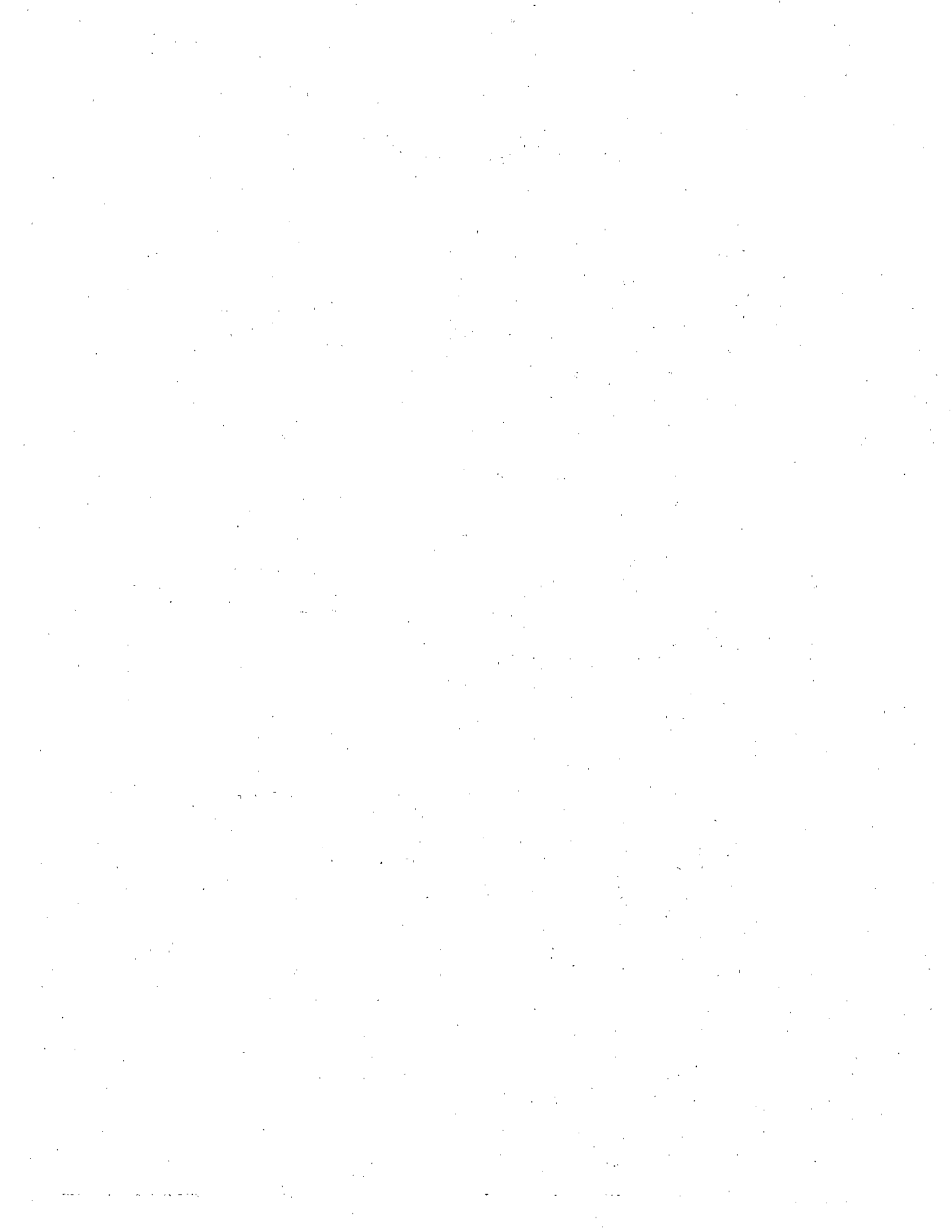
The maximum range for flyrock from vertical faces is controlled by a different set of conditions than the maximum range of flyrock from bench tops. In Section D-1 we will present methods of estimating flyrock range from vertical faces. Means of estimating flyrock range from bench tops will be given in Section D-2.

D-1 Flyrock Range from Vertical Faces

The information needed to estimate flyrock range from vertical faces is:

- a. Type of rock that is being blasted
- b. Diameter of borehole
- c. Burden to the free face at the top of the explosive column if the free face is inclined in the usual sense of a greater distance from borehole to the free face at the toe than at the collar
- d. Type of explosive in the main charge

Of the four items above only b) and d) are usually known precisely. It will be sufficiently accurate to classify rock types quite broadly, for example granite, limestone, sandstone, etc. It is very desirable to measure or estimate the minimum burden (item c) as accurately as possible. If vugs are noted in the free face, the horizontal distance between a neighboring borehole and the deepest portion of the vug should be used as the minimum burden if this distance is less than that defined in item c. The sketch below illustrates the determination of minimum burden, b, in the absence of vugs, and b' if there is a vug in the free face.



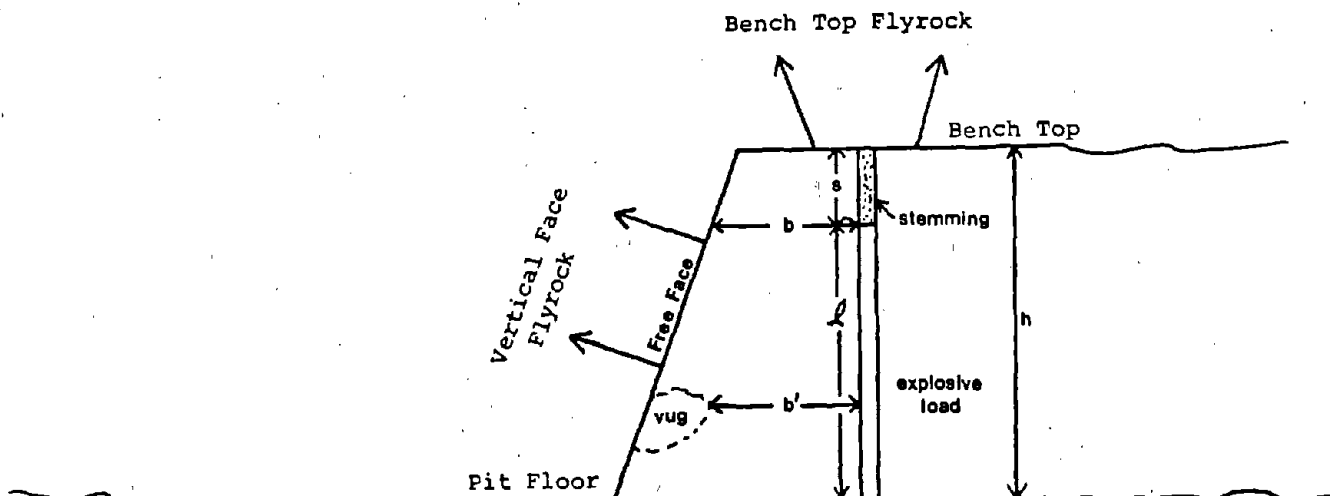


Figure 1-D: SKETCH OF A BENCH SHOT

In open pit mining most shots are fired with ANFO. In hard rock or under very wet conditions slurry explosives are also used. Thus, only ANFO or slurries will be considered in what follows. In fact, all the charts that follow are for ANFO-loaded shots. An approximate correction factor will be given to convert flyrock ranges for ANFO into flyrock ranges for slurry shots.

Figure 2-D gives the maximum flyrock range for flyrock from vertical faces for ANFO-loaded shots in granite. The plots in this chart can probably be also used to estimate flyrock ranges in other hard rock such as taconite or basalt.

Figure 3-D gives the maximum flyrock range for flyrock from vertical faces for ANFO-loaded shots in sandstone. The plots in this chart can probably be also used to estimate flyrock ranges in other soft material such as shale.

Figure 4-D gives the maximum flyrock range for flyrock from vertical faces for ANFO-loaded shots in limestone. The information upon which this chart was constructed is less accurate than that used in constructing Figures 2-D or 3-D.

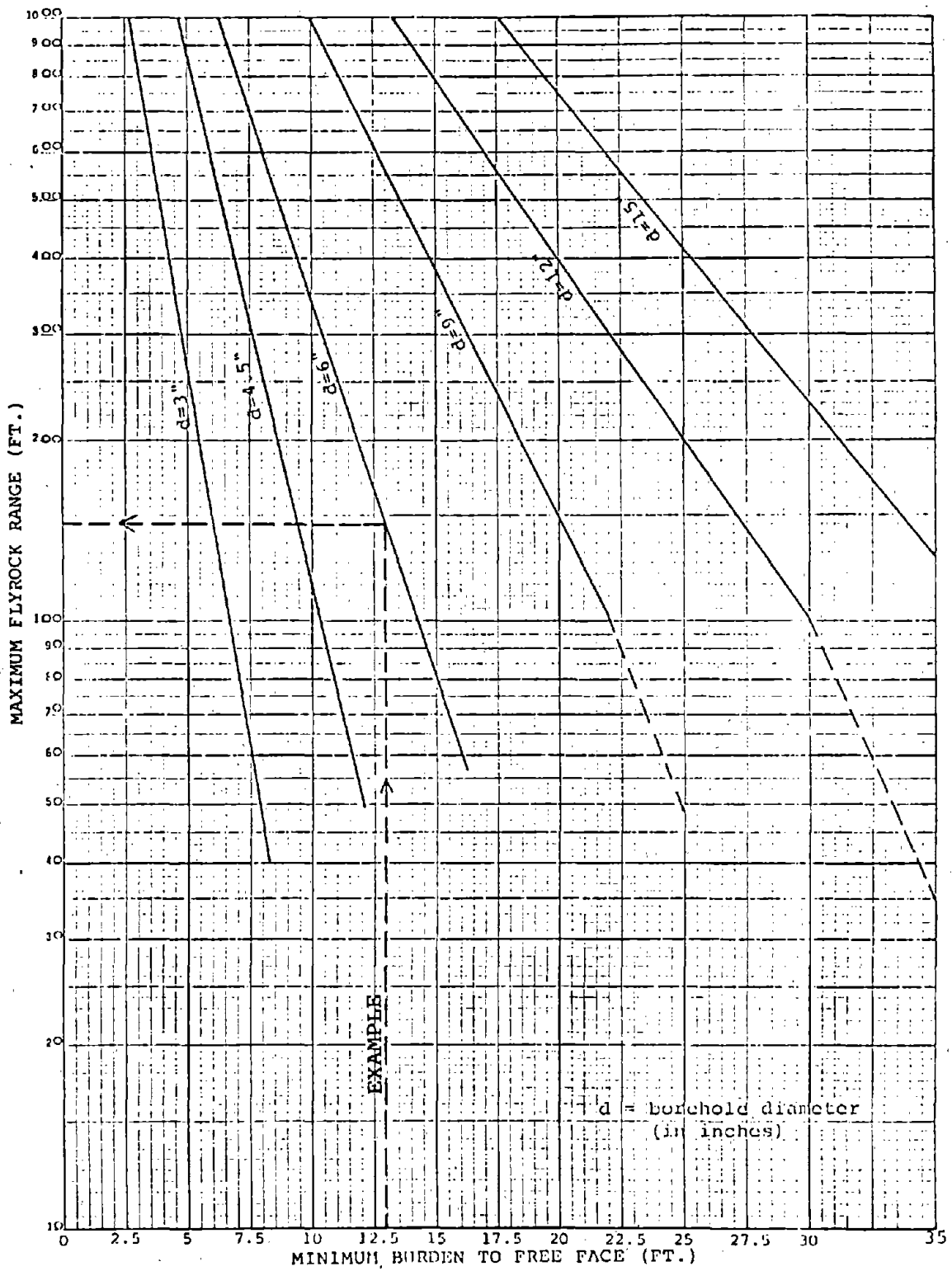


Figure 2-D: MAXIMUM RANGE OF VERTICAL FACE FLYROCK FROM ANFO-LOADED SHOTS IN GRANITE (FIXED BOREHOLE DIAMETERS)

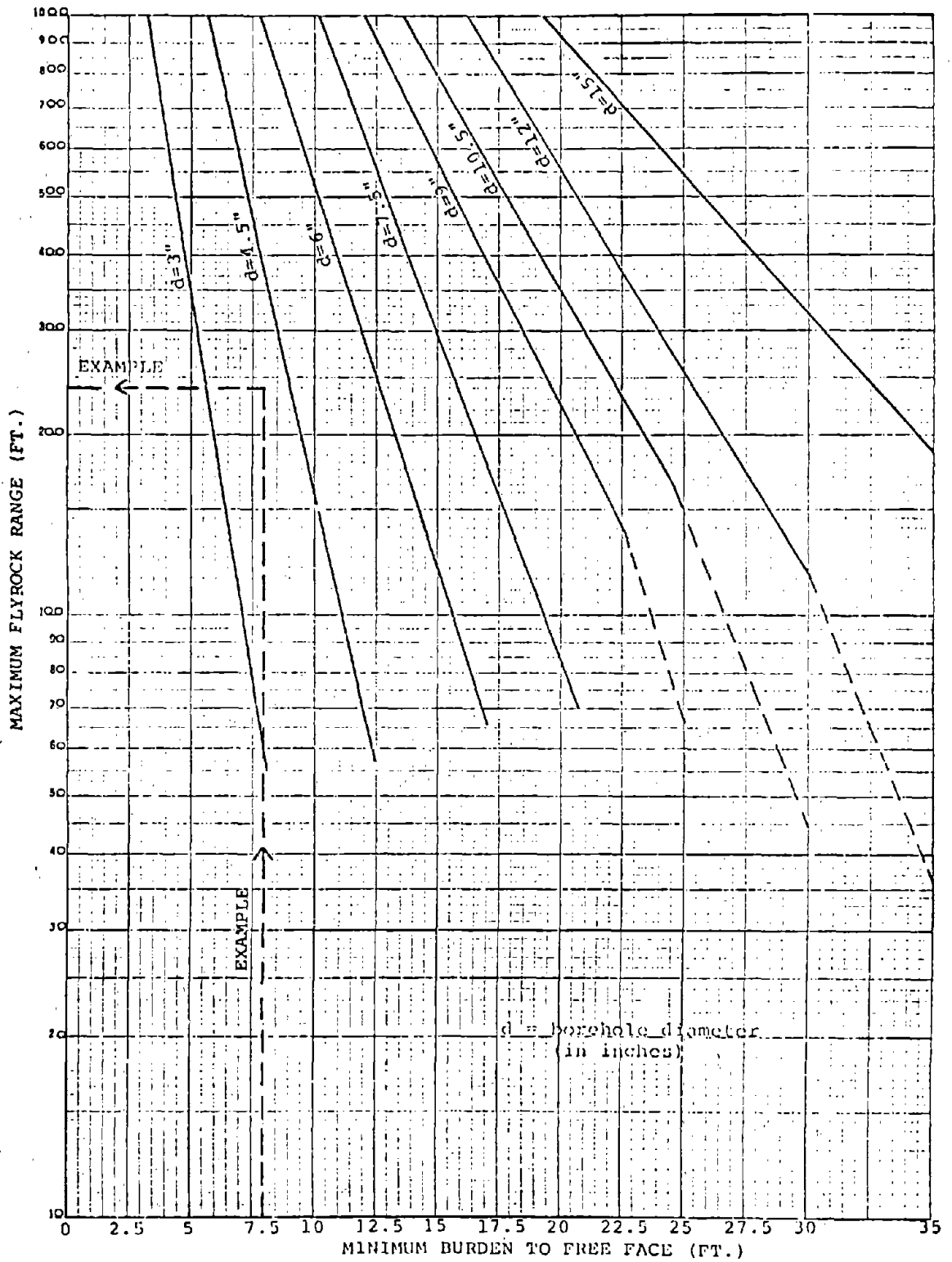


Figure 3-d: MAXIMUM RANGE OF VERTICAL FACE FLYROCK FROM ANFO-LOADED SHOTS IN SANDSTONE (FIXED BOREHOLE DIAMETERS)

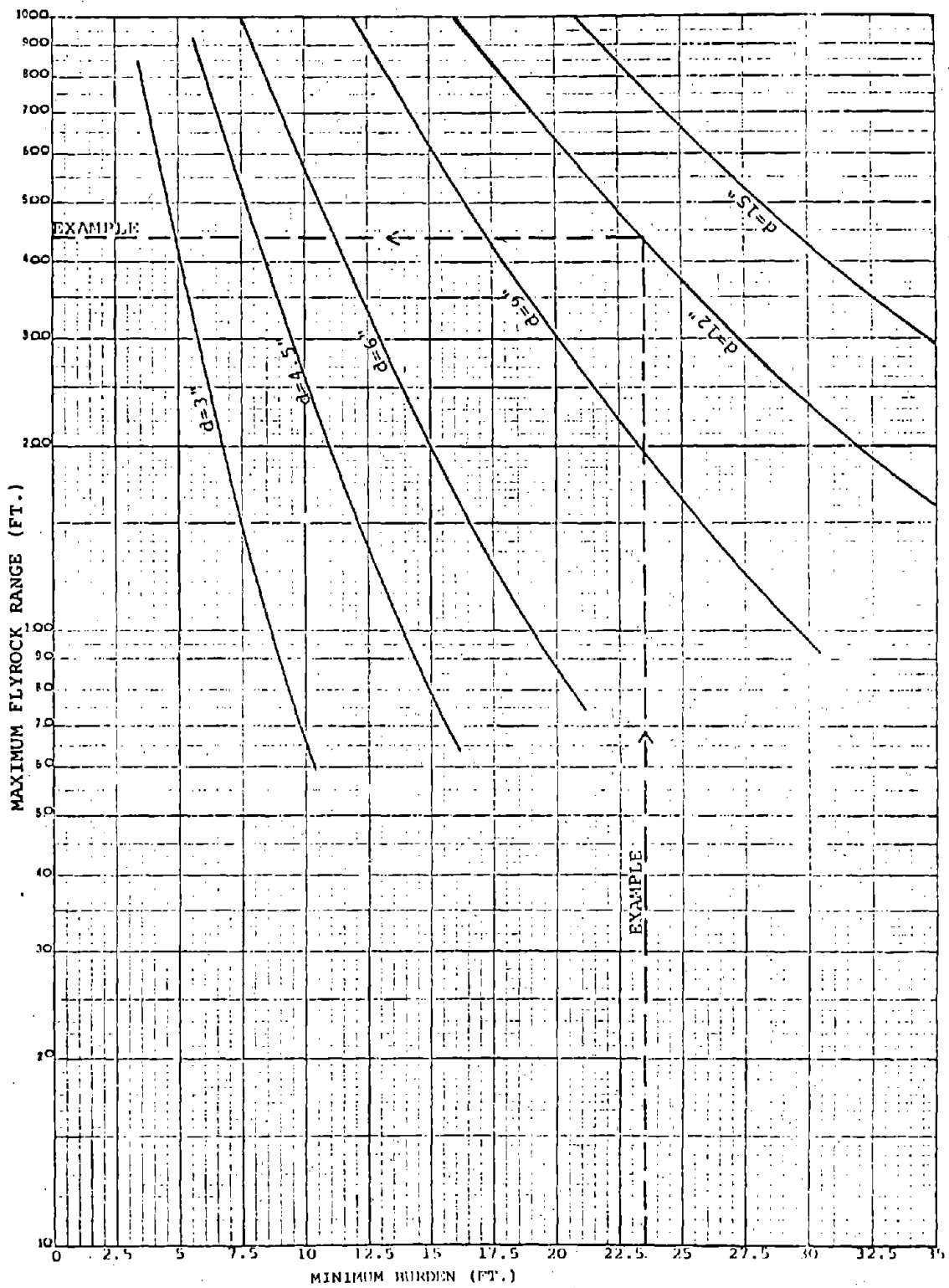


Figure 4-D: MAXIMUM RANGE OF VERTICAL FACE FLYROCK FROM ANFO-LOADED SHOTS IN LIMESTONE (FIXED BOREHOLE DIAMETER)

To illustrate the use of these charts, consider the following examples:

1. What is the maximum flyrock range for a shot in granite with 6 inch diameter boreholes loaded with ANFO and having a minimum burden of 13 feet?

Solution: In Figure 2-D go to the line labelled $d=6$ ". Find the vertical line which corresponds to a minimum burden of 13 feet. This line is one small division to the right of the line labelled 12.5 at the bottom of the chart. Move upward along this line to its intersection with the diagonal $d=6$ " line, as shown by the broken vertical line labelled "example". Move horizontally along the horizontal line passing through the intersection point until you reach the vertical scale at the left of the chart, as shown by the broken horizontal line labelled "example". Read a maximum flyrock range of 145 feet.

2. What is the maximum flyrock range for a shot in limestone with 12 inch diameter boreholes loaded with ANFO and having a minimum burden of 23.5 feet?

Solution: In Figure 4-D find the curve labelled $d=12$ ". Find the vertical line corresponding to a minimum burden of 23.5 feet. It is the line two small divisions to the right of the line labelled 22.5 feet at the bottom of the chart. Go up this line to its intersection with the $d=12$ " curve, as shown by the vertical broken line labelled "example". Go across along a horizontal line through this intersection to read 440 feet on the vertical scale on the left of the chart, as shown by the broken horizontal line. This is the answer sought.

3. What is the maximum flyrock range for a shot in sandstone with 4 inch diameter boreholes loaded with ANFO and having a minimum burden of 8 feet?

Approximate solution: In Figure 3-D find the vertical line corresponding to a minimum burden of 8 feet (one small division to the right of the line labelled 7.5 at the bottom of the chart). Move upwards along this line until it almost intersects the diagonal line labelled $d=4.5$ ". The exact position of this imaginary intersection is a "judgement call." In this example we will assume that this imaginary intersection occurs at a point given by the intersection of the broken vertical and horizontal lines shown. Move to the left along the broken horizontal line to read 240 feet on the vertical scale on the left on the chart.

More accurate solution: To facilitate estimation of flyrock range for borehole diameters not shown in Figures 2-D and 3-D, the information in these charts has been replotted in Figure 5-D for granite and Figure 6-D for sandstone. In the example considered, find the line corresponding to a borehole diameter of 4 inches at the bottom of Figure 6-D. Move vertically along this line to its intersection with the curve labelled $b=8'$. Move to the left along the horizontal line through this intersection to read 260 feet on the vertical scale on the left of the chart. This more accurate answer agrees fairly well with the 240 feet obtained by the approximate method above.

Many different types of slurry explosives are now used in production blasts. It would be time-consuming and confusing to have flyrock range charts for all these slurries. A reasonable estimate of the flyrock range of slurry-loaded shots can be obtained by simply multiplying the flyrock range of analogous ANFO-loaded shots by 1.5. Thus in example 1 if the boreholes were loaded with slurry, the flyrock range is about $1.5 \times 145 = 218$ feet; in example 2 it is $1.5 \times 440 = 660$ feet; in example 3 it is $1.5 \times 260 = 390$ feet.

D-2 Flyrock Range from Bench Tops

The information needed to estimate flyrock range from bench tops is:

- a. Weight of explosive per borehole, W
- b. Distance from the borehole collar to the top of the explosive charge, s (see Figure 1-D)
- c. Borehole diameter, d
- d. Type of rock being blasted
- e. Type of explosive used

As discussed in Section D-1, items c, d, and e are generally known precisely. Items a and b should be available from the shot loading plan and measurements during borehole loading. Rock

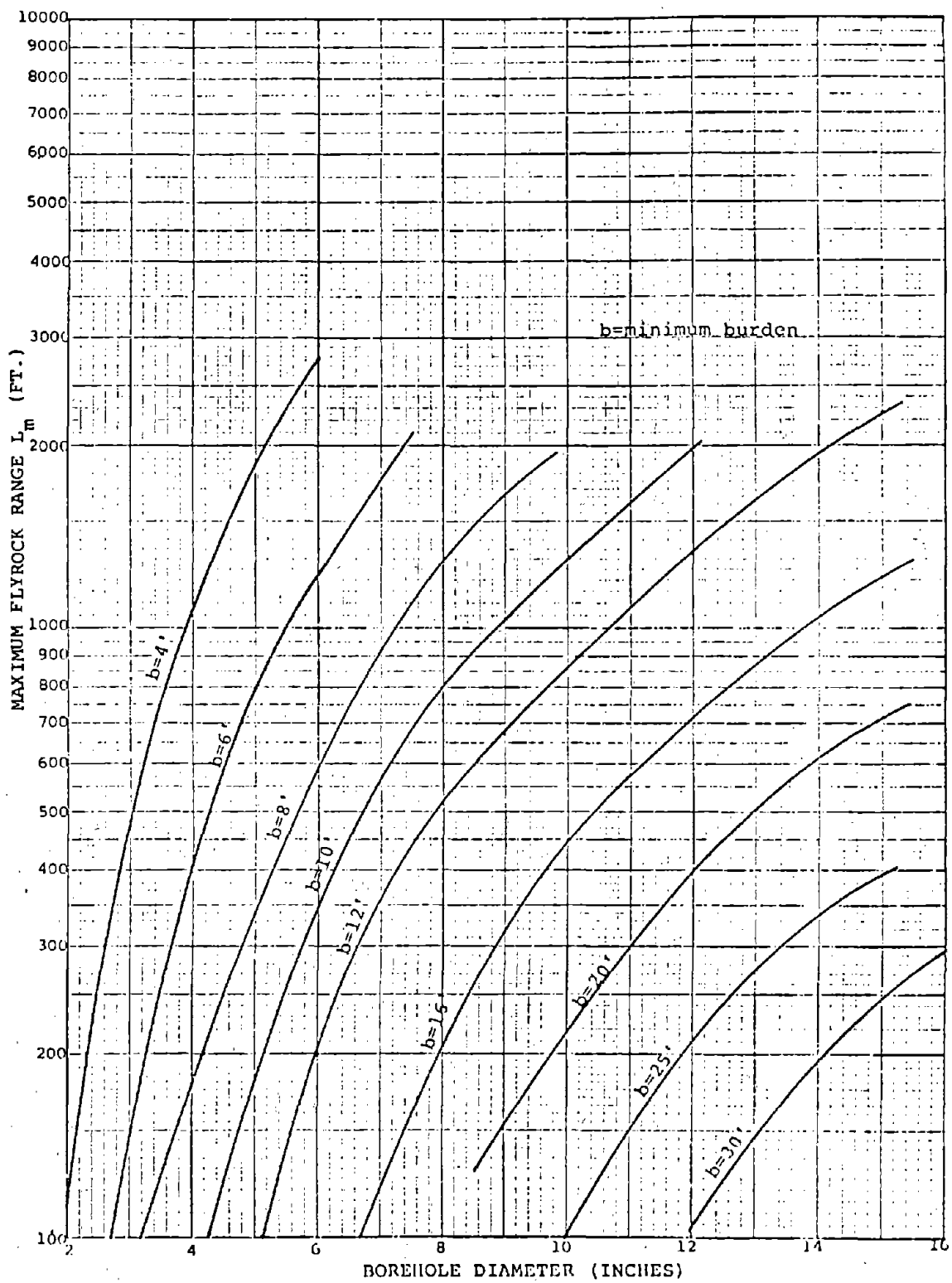


Figure 5-D: MAXIMUM RANGE OF VERTICAL FACE FLYROCK FROM ANFO-LOADED SHOTS IN GRANITE (FIXED BURDEN)

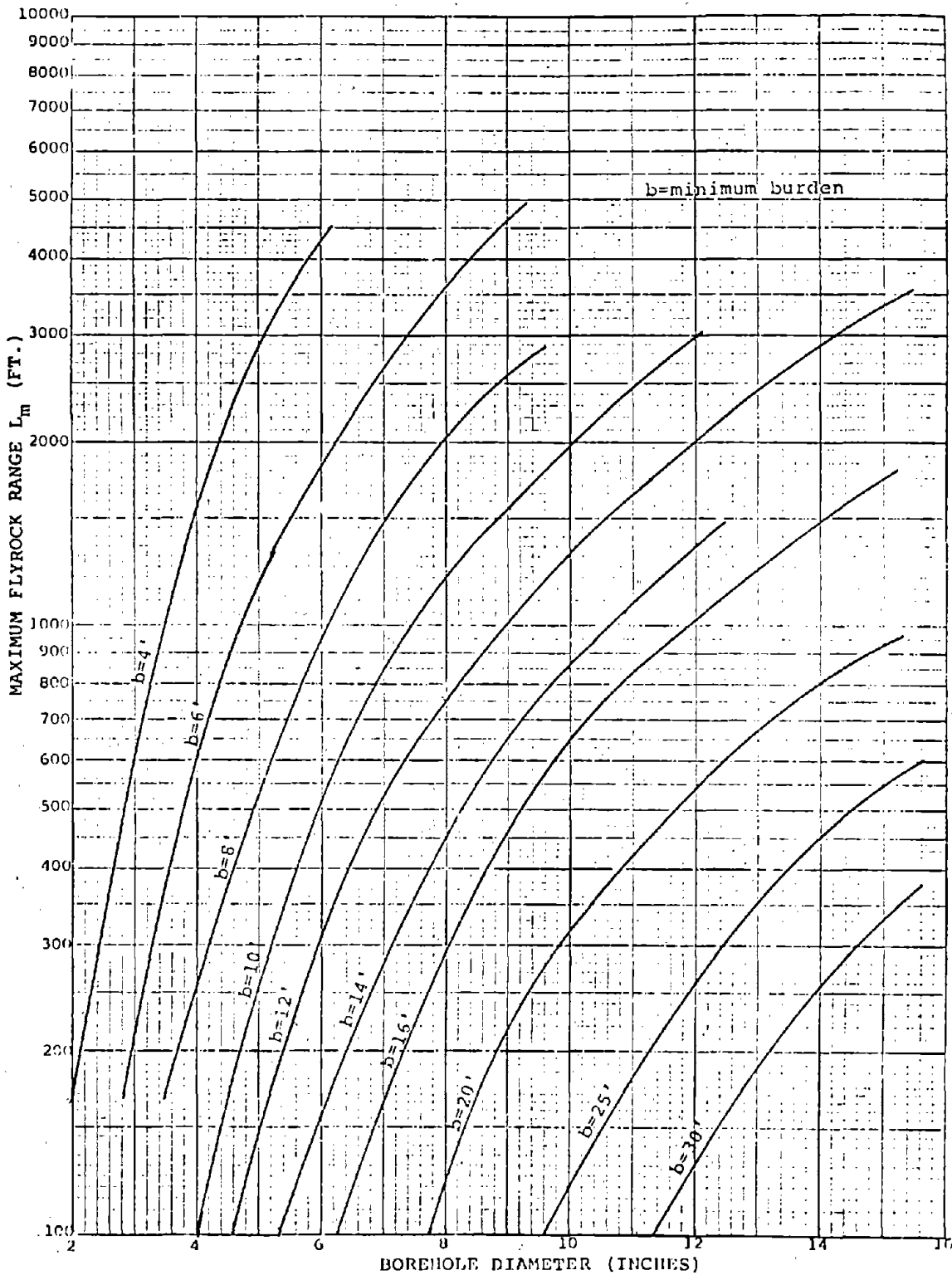


Figure 6-D: MAXIMUM RANGE OF VERTICAL FACE FLYROCK FROM ANFO-LOADED SHOTS IN SANDSTONE (FIXED BURDEN)

types can be grouped broadly as discussed in Section D-1. In what follows, the only type of explosive to be considered is ANFO. At present there is insufficient data to make precise estimates of the effect of using explosives other than ANFO except that in a general sense flyrock range is expected to be greater for slurry explosives than it is for ANFO.

It has been found that the factor that controls bench top flyrock range is $s/W^{1/3}$. This factor can be obtained from Figure 7-D.

Flyrock ranges for ANFO loaded shots in granite and sandstone are given in Figure 8-D as a function of the above factor ($s/W^{1/3}$) for three different borehole diameters. Flyrock ranges for limestone cannot at present be predicted with any degree of accuracy. However, in Figure 8-D at any value of $s/W^{1/3}$ they are expected to be roughly midway between the ranges for sandstone and granite.

The following examples will illustrate the use of this chart:

4. What is the maximum flyrock range of an ANFO shot in sandstone with 105 pounds of ANFO per 6 inch diameter borehole with 7 feet of stemming?

Solution: $W = 105$ lbs; $s = 7$ ft; $d = 6$ in. Enter Figure 7-D at $W = 105$ which is the imaginary vertical line midway between the vertical line labelled 100 at the bottom of the chart and the first small division to its right as indicated by the broken line in the chart. Proceed upward along this line labelled "example 4" to its intersection with diagonal line labelled $s = 7$ feet. Move to the left along the horizontal line through this intersection (as indicated by the broken line) to read $1.48 \text{ ft/lb}^{1/3}$ on the vertical scale on the left of the chart. Now enter Figure 8-D at $s/W^{1/3} = 1.48$ as shown by the broken vertical line labelled "example 4" and move to its intersection with the light diagonal line labelled $d=6"$. Move to the left along the horizontal line through this intersection (as shown) and read 170 feet on the vertical scale on the left of the chart. This is the answer sought.

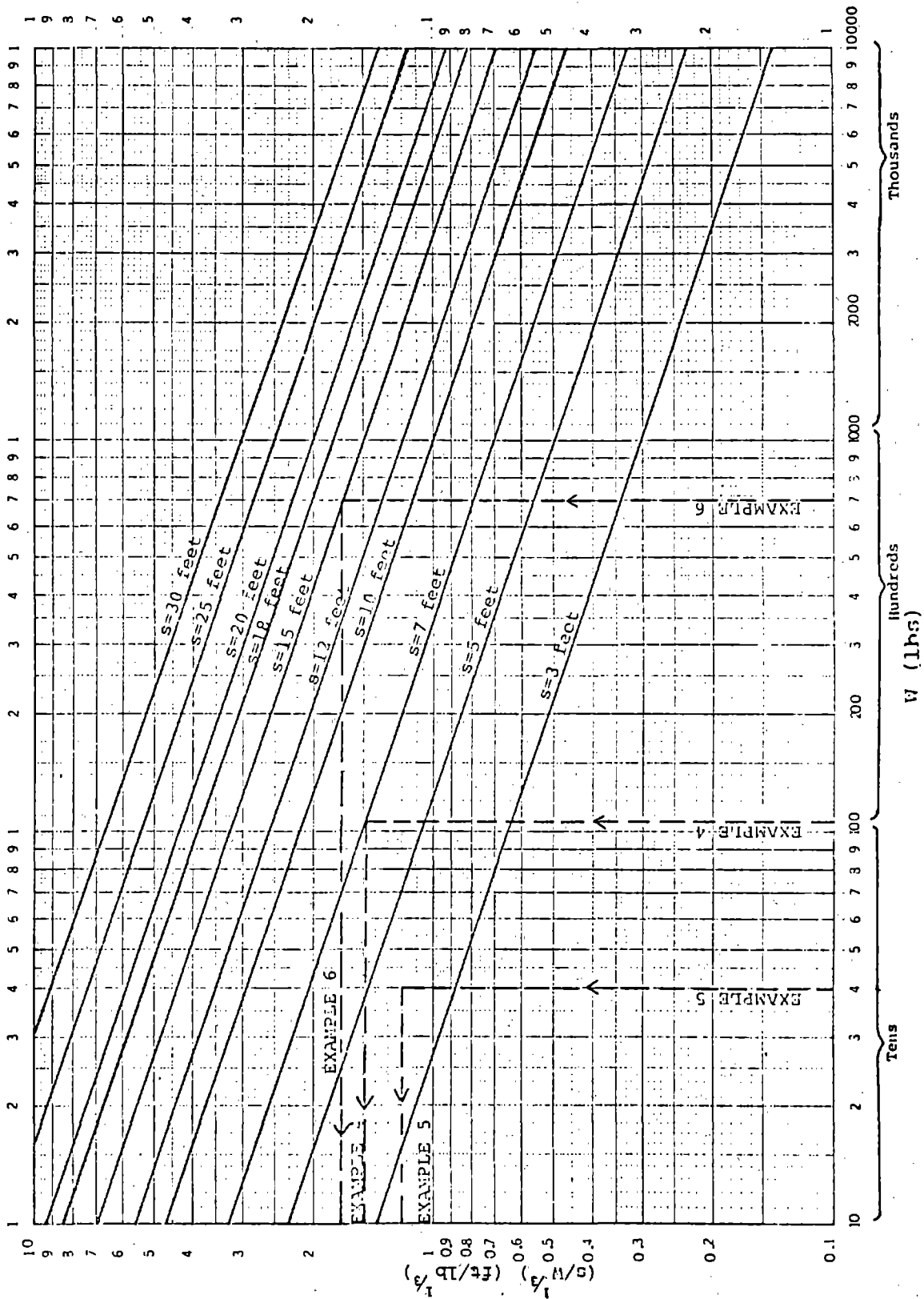


Figure 7-D: CORRELATION FACTOR ($s/W^{1/3}$) FOR BENCH TOP FLYROCK

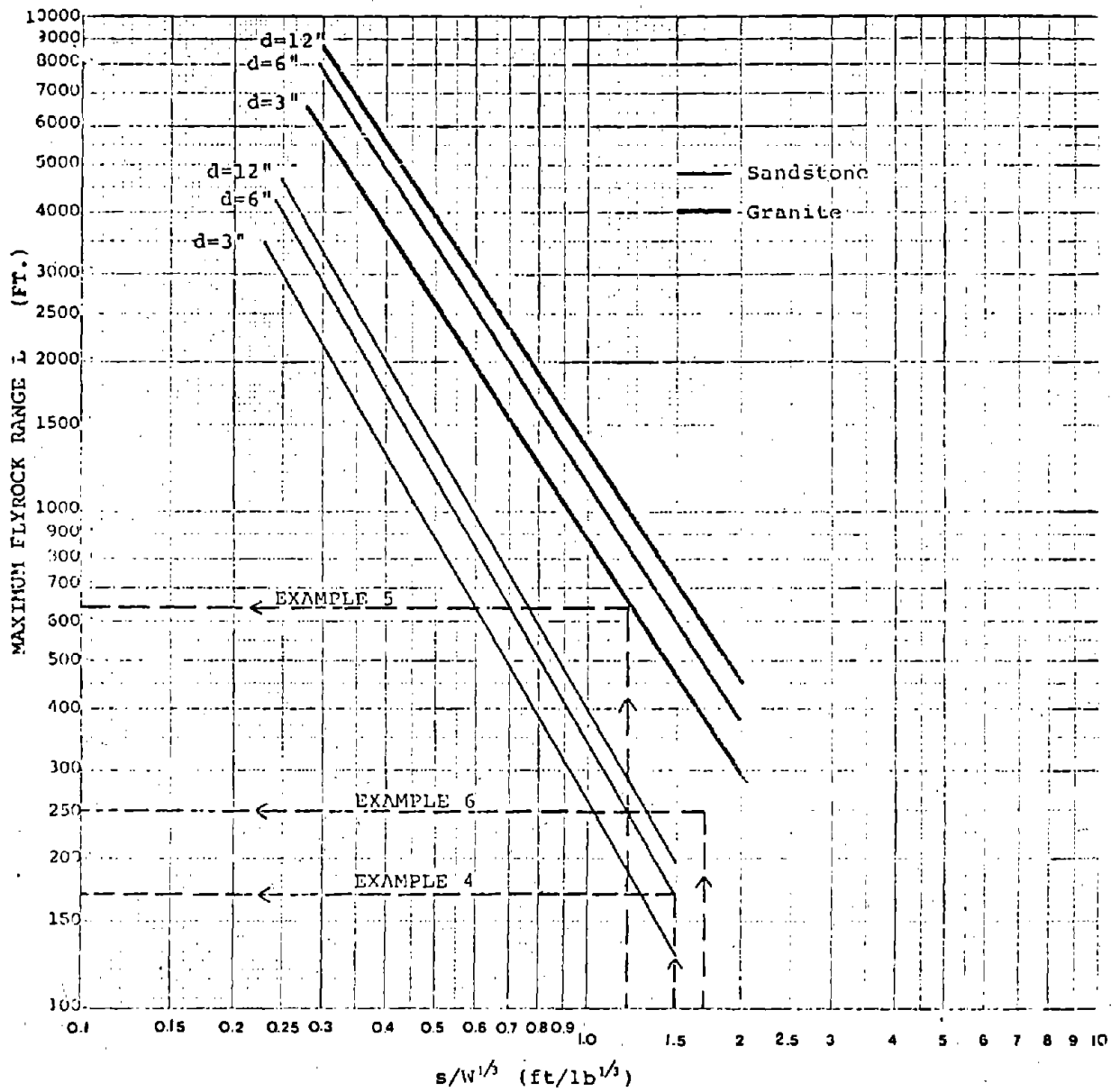


Figure 8-D: MAXIMUM RANGE FOR BENCH TOP FLYROCK FOR ANFO-LOADED SHOTS IN GRANITE AND SANDSTONE

5. What is the maximum flyrock range for an ANFO shot in granite with 40 pounds of ANFO per 3 inch diameter borehole with 4 feet of stemming?

Solution: $W = 40$ lbs; $s = 4$ ft; $d = 3$ in. Proceed as in example 4 along the broken lines in Figure 7-D labelled "example 5" to get $s/W^{1/3} = 1.2$ ft/lb^{1/3}. In Figure 8-D proceed along the broken lines labelled "example 5" to get a maximum flyrock range of 640 feet.

6. What is the maximum flyrock range for an ANFO shot in limestone with 700 pounds of ANFO per 6 inch diameter borehole with 15 feet of stemming?

Solution: $W = 700$ lbs; $s = 15$ ft; $d = 6$ in. Proceed as in example 4 along the broken line labelled "example 6" in Figure 7-D to get $s/W^{1/3} = 1.7$ ft/lb^{1/3}. Then in Figure 8-D proceed along the broken line labelled "example 6" to obtain an approximate flyrock range of 250 feet.

D-3 Elevation Correction

Flyrock from a tall bench (regardless of whether it originates from a free face or from a bench top) can travel further than flyrock from a low bench. The charts and examples of the preceding sections give flyrock range, L_m , for an imaginary bench that is at the same elevation as its surroundings. Normally benches are at an elevation that is higher than their surroundings. Thus a correction has to be applied to the flyrock ranges given in the preceding section to take into account the effect of higher elevation. The corrected flyrock range is given as a function of elevation above surroundings in Figure 9-D. The following examples will illustrate the use of this chart.

7. What is the maximum flyrock range of example 1 if the top of the explosive column is 50 feet above the surroundings (this is the distance labelled ℓ in Figure 1-D)?

Solution: Enter Figure 9-D at bottom at the vertical line labelled 50 feet. Proceed along this line (as

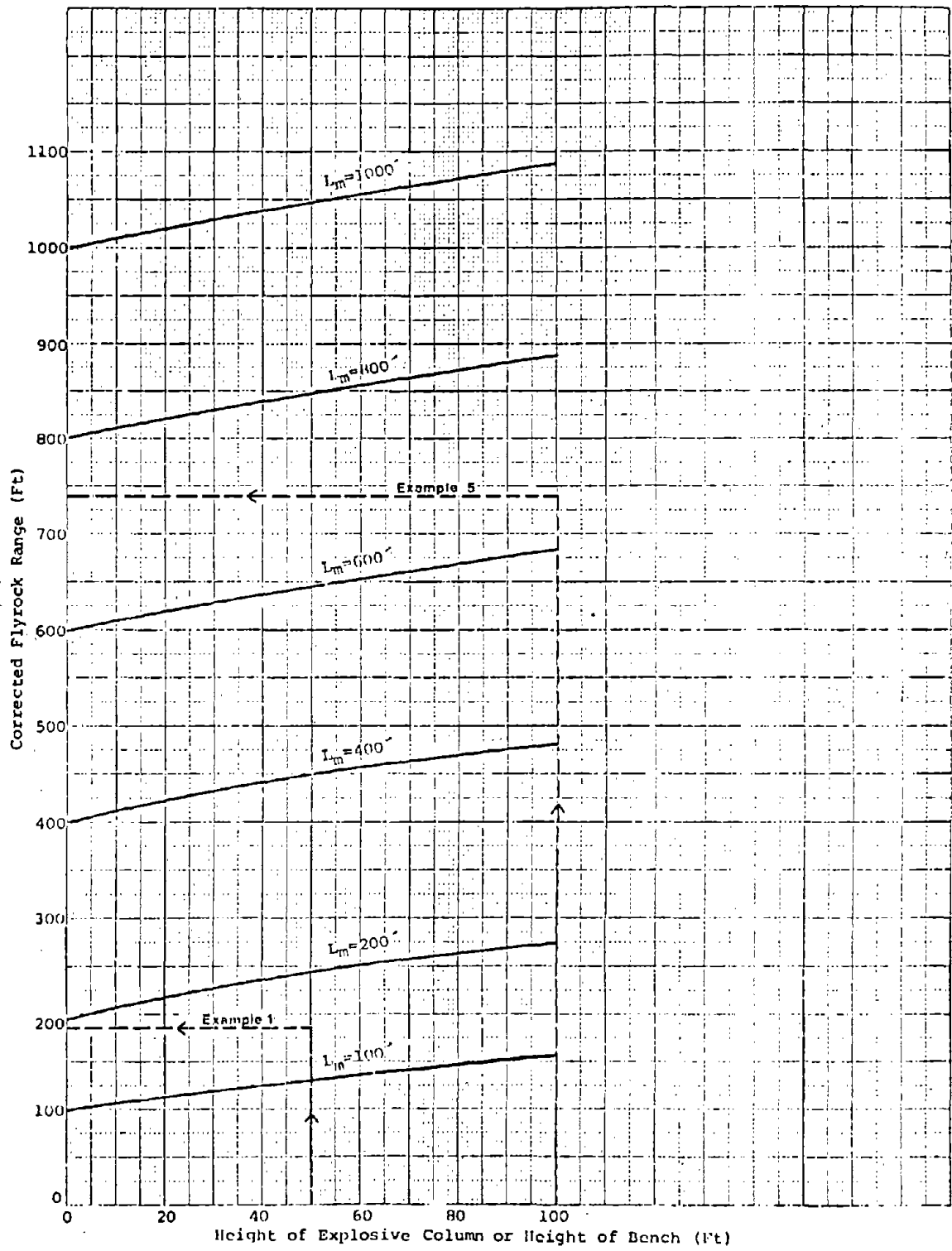


Figure 9-D: ELEVATION CORRECTION FOR MAXIMUM FLYROCK RANGE

shown by the broken line labelled "example 1") to a point about midway between the curves labelled $L_m = 100'$ and $L_m = 200'$ (since the $L_m = 145'$ obtained in example 1 is about halfway between 100' and 200') and then move horizontally to the left (as indicated by the broken line) to read a corrected flyrock range of 185 feet.

8. What is the maximum flyrock range of example 5 if bench is 100 feet above surroundings (height h in Figure 1-D)?

Solution: Enter Figure 9-D at bottom at the vertical line labelled 100'. Proceed as shown by the broken line labelled "example 5" to a point about one-quarter of the distance between the curves labelled $L_m = 600'$ and $L_m = 800'$ (L_m is 640' in example 5 or 40' above $L_m = 600'$. The difference between $L_m = 800'$ and $L_m = 600'$ is 200'; thus $40 \div 200$ is about one-quarter). Move horizontally to the left along broken line to read a corrected flyrock range of 740 feet.

As a general rule, elevation corrections for flyrock ranges are small if bench heights are small. Corrections are also relatively small if the uncorrected flyrock range (L_m) is already large.

APPENDIX E
SOME CONSIDERATIONS OF THE UTILIZATION OF EXPLOSIVE ENERGY
IN BREAKING ROCK

Although the utilization of explosive energy in rock blasting is only indirectly related to objectives of the present study, this is a subject of much interest and has received periodic attention over the years (References 8, 13, 15 and 26). Some of the deductions of the present study may cast additional light on this somewhat controversial matter and are consequently included in this report.

The model developed in the present study is capable of estimating the following:

- kinetic energy of the broken rock,
- kinetic energy of the detonation product gases,
- energy losses that do not contribute to propelling broken rock or product gases.

Presumably these energy losses consist of:

- residual energy in the product gases after they have expanded to a stage where they are no longer capable of breaking rock,
- gas venting losses through cracks or blown-out stemming,
- generation of seismic waves in the surrounding rock,
- crushing the rock immediately around the borehole,
- energy consumed in actually breaking the rock and related energy losses due to inter-rock friction as the rock breaks apart and/or losses due to plastic deformation of the rock.

Estimation of all these individual quantities is no simple task and, in fact, may be impossible with existing data. However, combining some of the loss terms simplifies the calculation and permits formulating some intriguing hypotheses concerning the optimum use of the chemical energy of the explosive for breaking rock in bench blasting.

Let us consider the energy used to break rock and to impart kinetic energy to the broken rock as "useful energy." The energy to crush rock around the borehole and to produce a seismic wave in the rock will be called "wasted energy." For the time being, we shall ignore "wasted energy" due to venting of detonation product gases. The kinetic energy of the broken rock is $mu_0^2/2$ and the work of breaking the rock (according to the model of Section 3.2.1) is mK_1W_r or simply mK' . The sum Σ of these two energies is:

$$\Sigma = m(u_0^2/2 + K'),$$

but from equation (12) $u_0^2 = S(c/m) - 2K'$, where S is the slope of the u_0^2 vs. c/m plot and $-2K'$ is the intercept. Consequently,

$$\Sigma = (m/2) [S(c/m) - 2K' + 2K'] = Sc/2. \quad (E-1)$$

The "useful energy" per unit weight of explosive, σ , is just $S/2$. The ratio of Σ to the total chemical energy cQ of the explosive is:

$$\Sigma/cQ = S/2Q. \quad (E-2)$$

The "wasted energy" per unit weight of explosive, according to Section 3.2.2 is $K_1W_s + K_2W_c = K''$. Now, from equation (12) $K''/E' = 1 - S/2E'$ and the ratio of "wasted energy" to the chemical energy of the explosive is:

$$K''/Q = E'/Q(1 - S/2E') = 2E'/2Q - S/2Q. \quad (E-3)$$

Now, we can examine the conditions for minimizing the ratio of "wasted energy" to "useful energy", namely K''/σ . From the above $K''/\sigma = (E' - S/2)/(S/2) = 2E'/S - 1$. Since $S = 2E'(1 - K''/E')$,

$$K''/\sigma = 1/(1 - K''/E') - 1 = (K''/E')/(1 - K''/E'). \quad (E-4)$$

According to equation (E-4), for a given rock (i.e., a given K''), K''/σ becomes progressively smaller as $2E'$ increases. Similarly, by eliminating S , $\sigma = 2E'(1 - K''/E')/2$ and σ , the useful work per unit weight of explosive increases as $2E'$ increases. Thus explosives with large values of $\sqrt{2E'}$ are expected to be more efficient than explosives with low $\sqrt{2E'}$.

Since imparting too much kinetic energy to the broken rock is undesirable (it creates far-ranging flyrock), optimum use of the chemical energy of the explosive is expected for explosives with large $2E'$ but with borehole diameters and burden to the free face chosen to keep c/m small. The factor $2E'$ can be increased by using an explosive whose detonation velocity, D , is large or an explosive whose Γ is small since $2E' = \text{const} [D^2 / (\Gamma - 1)]$. Thus, the effectiveness of the relatively low detonation velocity ANFO may be attributed to its low Γ .

We will use the vertical face data for granite to estimate an energy balance for rock blasting, since these data are the most extensive that we now have. Specifically we will use equation (13) in which all the data have been normalized to a $\sqrt{2E'}$ for EL506C sheet explosive. According to Reference 15, Q , the total chemical energy of this explosive is about 4×10^{10} ergs/g. The ratio of the kinetic energy of the broken rock to Q is given by $(m/c)(v_o^2/2Q)$. The ratio of the energy to break rock to Q is given by $(m/c)(K_3 W_r / 2Q)$. The tabulation below shows these rock kinetic energy and rock breakage energy ratios, as well as E/cQ , as a function of c/m .

$(c/m) 10^4$	$(m/c) 10^{-3}$	$m v_o^2 / 2cQ^*$	$m K_3 W_r / cQ^{**}$	E/cQ
2	5	0.071	0.365	0.436
3	3.33	0.192	0.244	0.436
5	2	0.290	0.146	0.436
10	1	0.363	0.073	0.436

* From equation (13)

** For $2K_3 W_r = 5.84 \times 10^6$ (cm/sec)²

As shown above, the sum of the two ratios is constant and independent of c/m . Thus, for the conditions described, the "useful energy" is about 44% of the chemical energy of the explosive.

According to equation (E-3) the energy that is used in generating the seismic wave in the rock plus the energy used in crushing the rock surrounding the borehole can be estimated as follows. Since $2E' = (2.3 \times 10^5)^2 \text{ (cm/sec)}^2$, $S = 3.478 \times 10^{10} \text{ (cm/sec)}^2$ and $Q = 4 \times 10^{10} \text{ ergs/g}$,

$$K''/Q = 0.226.$$

Thus, the energy consumed in imparting kinetic energy to the broken rock, breaking the rock, generating the seismic wave and crushing the rock around the borehole amounts to $0.436 + 0.226 = 0.662$ or about 2/3 of the chemical energy of the explosive. It may be expected that the remaining 1/3 of the chemical energy is "lost" through gas venting and residual energy of the product gases. However, this may not be the case.

Anderson²⁷ showed that the average escape velocity of product gases from a slab of explosive backed by a rigid boundary attains a maximum value of about $0.3D$, where D is the detonation velocity of the explosive. Thus, an extreme upper limit of the ratio of kinetic energy of the escaping gas to the chemical energy of the explosive (assuming that all the product gases vent) is $(0.3D)^2/2Q = 0.54$. Obviously this ratio is a gross overestimate, but it does suggest that appreciable energy can be lost through venting. These losses might be expected to be proportional to c , and thus be automatically included as an additional constant in the bracketed term of equation (12), and be part of what we have called seismic and crushing energies. However, these venting losses may differ not only for different strata but also for different explosives in the same strata. Thus the relation between venting losses and c may be quite complex.